tumors. Given that other *parkin*−/− mice did not develop HCC, the inconsistent phenotype observed by different laboratories might be due to differences in the genetic backgrounds of strains. Alternatively, the discrepancy between our results and those of others may have arisen from the timing of the analyses for the liver phenotype. Our *parkin*−/− mice model showed no evidence of hepatic tumors at 48 weeks. The majority of tumors were detected at an age of 72 weeks or older, whereas some of the previous analyses of *parkin*−/− mice were carried out when the mice were less than 72 weeks of age (Goldberg *et al.*, 2003; Palacino *et al.*, 2004). Further analyses are necessary to determine whether *parkin* deficiency is always responsible for enhanced hepatocyte proliferation and the development of HCC in various *parkin*−/− mouse models. In contrast to hepatomegaly, we found that the body weight of the *parkin*−/− mice was significantly lower than the wild-type mice by unknown reason. One possibility is to assume that changes in the levels of metabolism-related molecules were involved in the low body weights of *parkin*−/− mice.

Importantly, we demonstrated that *follistatin* is commonly upregulated in both nontumorous and tumorous liver tissues of *parkin*−/− mice. Our findings also showed that *parkin* expression resulted in the decrease in the expression levels of *follistatin* transcripts *in vitro*. The molecular mechanism responsible for regulation of *follistatin* transcription by parkin is unclear at present. However, it was shown that parkin regulates the gene transcription of monoamine oxidase in various cells (Jiang *et al.*, 2006). It is of note that the ability of parkin to suppress monoamine oxidase expression does not appear to be dependent on its ubiquitin ligase activity. Parc, a parkin-like ubiquitin ligase, also has a RING-IBR-RING motif and acts as a cytoplasmic anchor for the p53 protein, resulting in suppression of *p53* gene-dependent transcription (Nikolaev *et al.*, 2003). In the current study, reporter plasmid assay revealed that parkin expression induced the substantial decrease of promoter activity of *follistatin* gene. Thus, it might be possible to assume that parkin is involved in the transcriptional regulation of *follistatin* gene expression, either independent of its E3 ligase function or by the proteosomal degradation of the target protein related to the transcriptional regulation of *follistatin*. In addition to the possible transcriptional regulation of *follistatin* by parkin, the activation of β-catenin observed in the HCC tissues might be attributable to enhanced expression of the *follistatin* gene, because it has been demonstrated that activation of β-catenin results in the induction of *follistatin* expression in various cancer cells (Willert *et al.*, 2002; Germann *et al.*, 2003).

Our data showed that *parkin*−/− hepatocytes were significantly more resistant to cell death in association with the upregulation of *follistatin*. Follistatin is secreted, and is sometimes membrane associated, and exerts its effects as the most potent endogenous inhibitor of activin (Harrison *et al.*, 2005). Accumulating evidence suggests that the activin/follistatin system is involved in the regulation of hepatocyte proliferation and apoptotic cell death (Chen *et al.*, 2002; Harrison *et al.*, 2005; Rodgarkia-Dara *et al.*, 2006). Several animal models and analyses of clinical specimens revealed that deregulation of activin signaling, mainly achieved by follistatin upregulation, contributes to pathologic conditions such as hepatic inflammation, fibrosis and liver cancer (Rossmanith *et al.*, 2002; Grusch *et al.*, 2006; Patella *et al.*, 2006). Overexpression of activins induces hepatocyte apoptosis *in vitro* and *in vivo* (Schwall *et al.*, 1993; Hully *et al.*, 1994), whereas follistatin administration decreased hepatocyte apoptosis in a hepatitis mouse model (Patella *et al.*, 2006). Furthermore, follistatin administration by intraportal infusion or adenovirus-mediated overexpression stimulates DNA synthesis and liver growth in normal rat livers (Kogure *et al.*, 2000; Takabe *et al.*, 2003). Experimentally induced rodent liver tumors, as well as human HCCs, show upregulated expression of *follistatin* (Grusch *et al.*, 2006). These findings suggest that deregulation of the balance between the expression of activins and their antagonist, follistatin, may contribute to the growth advantage of hepatocytes and result in liver cancer. Therefore, it is likely that upregulation of *follistatin* is associated with the development of HCC in *parkin*−/− mice.

In conclusion, our findings demonstrate that parkin is important in the regulation of hepatocyte proliferation and apoptosis, and that the loss of parkin expression might contribute to the overproliferation of hepatocytes, leading to hepatocarcinogenesis. Because β-catenin activation was specifically observed in the tumor, but not in the nontumorous region of the *parkin*-deficient livers, additional events for genetic changes might be required in the *parkin*-deficient liver to develop the HCC.

Materials and methods

Generation of parkin−/− *mice*

The mutant *parkin* allele lacking approximately 2 kb of the *parkin* exon 3 genomic sequence was generated in a mixed 129SV/C57BL6 (50/50) genetic background (Kitao *et al.*, 2007). Mice received humane care according to the *Guide for the Care and Use of Laboratory Animals* prepared by the National Academy of Sciences and published by the National Institutes of Health (NIH publication 86–23).

Isolation and culture of mouse primary hepatocytes

Mouse primary hepatocytes were obtained from 10- to 11-week-old mice by the two-step collagenase perfusion method (Seglen, 1976). In brief, hepatocyte suspensions were obtained by passing collagenase type II (Gibco BRL, Life Technologies Inc., Rockville, MD, USA) digested liver through a 70 μm cell strainer, followed by centrifugation to collect the mature hepatocytes. After isolation, hepatocytes were resuspended in Dulbecco's modified Eagle's medium (DMEM; Gibco-BRL) supplemented with 10% fetal bovine serum and seeded on collagen type I-coated dishes at a density of 8×10^4 cells/cm^2. The cells were maintained at 37 °C in a humidified atmosphere of 5% CO_2.

siRNA duplexes composed of 25 nucleotide sense and antisense strands used for targeting follistatin were obtained

from Invitrogen (Carlsbad, CA, USA). siRNA (20 μM) in 60 μl of Trans-IT-TKO reagent (Mirus Bio Corporation, Madison, WI, USA) was incubated in serum-free Opti-MEM medium (Qiagen, Valencia, CA, USA) for 10 min, followed by the addition of transfection mixture into the cells.

Quantitative real-time RT–PCR
RNA was extracted using Sepasol-RNA 1 Super (Nacalai Tesque, Kyoto, Japan). For the RT reaction, total RNA was reverse-transcribed into cDNA using the Superscript III first strand synthesis system and oligo-dT_{12-18} primers (Invitrogen; Matsumoto *et al.*, 2006). PCR amplification was performed using Takara Ex Taq DNA polymerase (Takara, Tokyo, Japan). The oligonucleotide primers used in this study are shown in Supplementary Table 4. Quantification of gene expression was performed by quantitative real-time RT–PCR using a 7300 Real-Time PCR system (PE Applied Biosystems, Foster City, CA, USA) and Platinum SYBR Green qPCR SuperMix UDG (Invitrogen) as described (Kou *et al.*, 2006). To assess the quantity of isolated RNA, as well as the efficiency of cDNA synthesis, target cDNAs were normalized to the endogenous mRNA levels of the housekeeping reference gene, *18S rRNA* (Matsumoto *et al.*, 2006). For simplicity, the expression levels of the target gene were expressed relative to those of the control specimen. Human liver tissues for RT–PCR analyses were obtained from biopsy specimens of tumor tissues at the proximal edge of freshly resected specimens and frozen immediately in liquid nitrogen.

RNA preparation and hybridization to the microarray
Total RNA was extracted from mice liver tissues using a RNA assay mini kit (Qiagen). First-strand cDNA was synthesized from 500 ng of total RNA in the presence of Cy5 or Cy3 dCTP. The Cy3- and Cy5-labeled samples derived from wild-type and *parkin−/−* mice at 72 weeks of age were injected simultaneously into the same spot of the whole mouse 60-mer oligo microarray (Agilent Technologies, Palo Alto, CA, USA). After hybridization at 65 °C for 17 h, the slides were washed with 6× SSC containing 0.005% Triton X-102, and dried using a nitrogen-filled air gun. Array image acquisition and feature extraction was performed using an Agilent G2565AA Microarray Scanner with feature extraction software (version 8.5.1.1; Agilent Technologies). Statistical evaluation was performed using the algorithm developed by Agilent for the array analysis. Genes that were upregulated or downregulated in tumorous and nontumorous liver tissues by more than fivefold compared to normal liver tissues and had *P*-values less than 0.05 were considered.

Immunoblotting analysis
Protein samples were separated by SDS–polyacrylamide gel electrophoresis (PAGE) 10% (w/v) polyacrylamide gels and subjected to immunoblotting analysis as described previously (Endo *et al.*, 2007). The polyclonal antibodies against mouse follistatin and α-tubulin were purchased from Santa Cruz Biotechnology (Santa Cruz, CA, USA) and Calbiochem (San Diego, CA, USA), respectively.

Immunohistochemical staining analysis
Immunohistochemical staining was carried out according to a previously described protocol (Toda *et al.*, 1999). The polyclonal antibodies for PCNA, AFP and β-catenin were purchased from Santa Cruz Biotechnology, Dako Cytomation (Glostrup, Denmark) and Transduction Labs (Palo Alto, CA, USA), respectively.

Measurement of caspase activity and apoptosis assay
Liver tissues from the mice were prepared in buffer A (1 M KCl, 1 M $MgCl_2$, 1 M 4-(2-hydroxyethyl)-1-piperazineethanesulfonic acid, 0.5 M EDTA and 10% CHAPS) and normalized for total protein content. A 30 μg sample of protein was incubated with either 10 ng of granzyme B (Calbiochem) or 0.5 nmol of cytochrome *c* (Sigma, St Louis, MO, USA) and 1 mM dATP at 37 °C for 30 min as described (Marusawa *et al.*, 2003). Then, 5 μl of reaction mixture was incubated with caspase-3 substrate Ac-DEVD-pNA (10 mM), and caspase activity was assessed using a colorimetric CaspACE assay system (Promega, Madison, WI, USA). For the measurement of caspase-3 activity, the plates were read at 405 nm using microplate reader (Molecular Devices Co., Tokyo, Japan). For the evaluation of cell death, mice primary hepatocytes were cultured in DMEM on collagen-coated dishes. After 24 h of isolation, cells were treated with either CDDP (200 μM), DOX (10 μM) or VP-16 (400 nM) for 48 h. Cell viability was determined by the trypan blue exclusion test (Marusawa *et al.*, 2003) or the Annexin-V-Fluos apoptosis detection kit (Roche Applied Science, Indianapolis, IN, USA) according to the manufacturer's instruction.

Flow cytometric analysis
A total of 1×10^5 cells were plated on 10 cm collagen-coated dishes. Two days after treatment with HGF (PeproTech, London, UK) at a concentration of 10 ng/ml, BrdU (20 μM; Roche, Basel, Switzerland) was added to the culture medium for 12 h. The cells were then fixed in 70% ice-cold ethanol and incubated at 4 °C overnight. Fluorescence was determined by using a FACScan flow cytometer (Becton Dickinson, Franklin Lake, NJ, USA) after adding propidium iodide. Data were acquired and analysed using CELLQuest software (Becton Dickinson).

Cell culture, transfection and reporter plasmid assay
Human hepatoma-derived cell lines, Huh-7 and Hep3B were maintained in DMEM containing 10% fetal bovine serum. For plasmid transfection, we used Lipofectamine (Invitrogen) for Huh-7 and Trans-IT 293 (Mirus Bio Corporation) for Hep3B. To determine the promoter activity of the *follistatin* gene, the reporter plasmids were generated by inserting the PCR-amplified 196- and 361-bp 5′-proximal promoter regions of the *follistatin* gene (de Groot *et al.*, 2000) into the pGL-3 luciferase vectors (Promega). The reporter construct and pRL-TK (Promega) were then co-transfected with an expression plasmid-encoding *parkin* or control vector into NIH3T3 cells. The cell lysates were analysed for luciferase activity using the Dual-Luciferase Reporter Assay System (Promega; Tanaka *et al.*, 2006).

Acknowledgements

We thank Dr T Fukushima for flow cytometric analysis, and Dr H Hiai for useful comments on histological study. This work was supported by Grants-in-Aid for Scientific Research 16017240, 15209024 and 15659169 from the Ministry of Education, Culture, Sports, Science, and Technology of Japan, and Grant-in-Aid for Research on Measures for Intractable Diseases, and Research on Advanced Medical Technology from the Ministry of Health, Labor, and Welfare, Japan.

References

Cesari R, Martin ES, Calin GA, Pentimalli F, Bichi R, McAdams H *et al.* (2003). Parkin, a gene implicated in autosomal recessive juvenile parkinsonism, is a candidate tumor suppressor gene on chromosome 6q25–q27. *Proc Natl Acad Sci USA* **100**: 5956–5961.

Chen YG, Lui HM, Lin SL, Lee JM, Ying SY. (2002). Regulation of cell proliferation, apoptosis, and carcinogenesis by activin. *Exp Biol Med (Maywood)* **227**: 75–87.

Dawson TM, Dawson VL. (2003). Molecular pathways of neurodegeneration in Parkinson's disease. *Science* **302**: 819–822.

De Groot E, Veltmaat J, Caricasole A, Defize L, van den Eijnden-van Raaij A. (2000). Cloning and analysis of the mouse follistatin promoter. *Mol Biol Rep* **27**: 129–139.

Denison SR, Wang F, Becker NA, Schule B, Kock N, Phillips LA *et al.* (2003). Alterations in the common fragile site gene Parkin in ovarian and other cancers. *Oncogene* **22**: 8370–8378.

Endo Y, Marusawa H, Kinoshita K, Morisawa T, Sakurai T, Okazaki IM *et al.* (2007). Expression of activation-induced cytidine deaminase in human hepatocytes via NF-kappa B signaling. *Oncogene* **26**: 5587–5595.

Farazi PA, DePinho RA. (2006). Hepatocellular carcinoma pathogenesis: from genes to environment. *Nat Rev Cancer* **6**: 674–687.

Farrer MJ. (2006). Genetics of Parkinson disease: paradigm shifts and future prospects. *Nat Rev Genet* **7**: 306–318.

Feitelson MA, Sun B, Satiroglu Tufan NL, Liu J, Pan J, Lian Z. (2002). Genetic mechanisms of hepatocarcinogenesis. *Oncogene* **21**: 2593–2604.

Germann A, Dihlmann S, Hergenhahn M, Doeberitz MK, Koesters R. (2003). Expression profiling of CC531 colon carcinoma cells reveals similar regulation of beta-catenin target genes by both butyrate and aspirin. *Int J Cancer* **106**: 187–197.

Goldberg MS, Fleming SM, Palacino JJ, Cepeda C, Lam HA, Bhatnagar A *et al.* (2003). Parkin-deficient mice exhibit nigrostriatal deficits but not loss of dopaminergic neurons. *J Biol Chem* **278**: 43628–43635.

Grusch M, Drucker C, Peter-Vorosmarty B, Erlach N, Lackner A, Losert A *et al.* (2006). Deregulation of the activin/follistatin system in hepatocarcinogenesis. *J Hepatol* **45**: 673–680.

Hahn WC, Weinberg RA. (2002). Rules for making human tumor cells. *N Engl J Med* **347**: 1593–1603.

Harrison CA, Gray PC, Vale WW, Robertson DM. (2005). Antagonists of activin signaling: mechanisms and potential biological applications. *Trends Endocrinol Metab* **16**: 73–78.

Hully JR, Chang L, Schwall RH, Widmer HR, Terrell TG, Gillett NA. (1994). Induction of apoptosis in the murine liver with recombinant human activin A. *Hepatology* **20**: 854–862.

Itier JM, Ibanez P, Mena MA, Abbas N, Cohen-Salmon C, Bohme GA *et al.* (2003). Parkin gene inactivation alters behaviour and dopamine neurotransmission in the mouse. *Hum Mol Genet* **12**: 2277–2291.

Jackson PK, Eldridge AG, Freed E, Furstenthal L, Hsu JY, Kaiser BK *et al.* (2000). The lore of the RINGs: substrate recognition and catalysis by ubiquitin ligases. *Trends Cell Biol* **10**: 429–439.

Jiang H, Jiang Q, Liu W, Feng J. (2006). Parkin suppresses the expression of monoamine oxidases. *J Biol Chem* **281**: 8591–8599.

Kahle PJ, Haass C. (2004). How does parkin ligate ubiquitin to Parkinson's disease? *EMBO Rep* **5**: 681–685.

Kitada T, Asakawa S, Hattori N, Matsumine H, Yamamura Y, Minoshima S *et al.* (1998). Mutations in the parkin gene cause autosomal recessive juvenile parkinsonism. *Nature* **392**: 605–608.

Kitao Y, Imai Y, Ozawa K, Kataoka A, Ikeda T, Soda M *et al.* (2007). Pael receptor induces death of dopaminergic neurons in the substantia nigra via endoplasmic reticulum stress and dopamine toxicity, which is enhanced under condition of parkin inactivation. *Hum Mol Genet* **16**: 50–60.

Kogure K, Zhang YQ, Maeshima A, Suzuki K, Kuwano H, Kojima I. (2000). The role of activin and transforming growth factor-beta in the regulation of organ mass in the rat liver. *Hepatology* **31**: 916–921.

Kong FM, Anscher MS, Washington MK, Killian JK, Jirtle RL. (2000). M6P/IGF2R is mutated in squamous cell carcinoma of the lung. *Oncogene* **19**: 1572–1578.

Kou T, Marusawa H, Kinoshita K, Endo Y, Okazaki IM, Ueda Y *et al.* (2006). Expression of activation-induced cytidine deaminase in human hepatocytes during hepatocarcinogenesis. *Int J Cancer* **120**: 469–476.

Laurent-Puig P, Zucman-Rossi J. (2006). Genetics of hepatocellular tumors. *Oncogene* **25**: 3778–3786.

Lengauer C, Kinzler KW, Vogelstein B. (1998). Genetic instabilities in human cancers. *Nature* **396**: 643–649.

Marusawa H, Matsuzawa S, Welsh K, Zou H, Armstrong R, Tamm I *et al.* (2003). HBXIP functions as a cofactor of survivin in apoptosis suppression. *EMBO J* **22**: 2729–2740.

Matsumoto T, Marusawa H, Endo Y, Ueda Y, Matsumoto Y, Chiba T. (2006). Expression of APOBEC2 is transcriptionally regulated by NF-kappaB in human hepatocytes. *FEBS Lett* **580**: 731–735.

Millikin D, Meese E, Vogelstein B, Witkowski C, Trent J. (1991). Loss of heterozygosity for loci on the long arm of chromosome 6 in human malignant melanoma. *Cancer Res* **51**: 5449–5453.

Morett E, Bork P. (1999). A novel transactivation domain in parkin. *Trends Biochem Sci* **24**: 229–231.

Morita R, Saito S, Ishikawa J, Ogawa O, Yoshida O, Yamakawa K *et al.* (1991). Common regions of deletion on chromosomes 5q, 6q, and 10q in renal cell carcinoma. *Cancer Res* **51**: 5817–5820.

Negrini M, Sabbioni S, Possati L, Rattan S, Corallini A, Barbanti-Brodano G *et al.* (1994). Suppression of tumorigenicity of breast cancer cells by microcell-mediated chromosome transfer: studies on chromosomes 6 and 11. *Cancer Res* **54**: 1331–1336.

Nikolaev AY, Li M, Puskas N, Qin J, Gu W. (2003). Parc: a cytoplasmic anchor for p53. *Cell* **112**: 29–40.

Palacino JJ, Sagi D, Goldberg MS, Krauss S, Motz C, Wacker M *et al.* (2004). Mitochondrial dysfunction and oxidative damage in parkin-deficient mice. *J Biol Chem* **279**: 18614–18622.

Patella S, Phillips DJ, Tchongue J, De Kretser DM, Sievert W. (2006). Follistatin attenuates early liver fibrosis: effects on hepatic stellate cell activation and hepatocyte apoptosis. *Am J Physiol Gastrointest Liver Physiol* **290**: G137–G144.

Perez FA, Palmiter RD. (2005). Parkin-deficient mice are not a robust model of parkinsonism. *Proc Natl Acad Sci USA* **102**: 2174–2179.

Picchio MC, Martin ES, Cesari R, Calin GA, Yendamuri S, Kuroki T *et al.* (2004). Alterations of the tumor suppressor gene Parkin in non-small cell lung cancer. *Clin Cancer Res* **10**: 2720–2724.

Rodgarkia-Dara C, Vejda S, Erlach N, Losert A, Bursch W, Berger W *et al.* (2006). The activin axis in liver biology and disease. *Mutat Res* **613**: 123–137.

Rodriguez C, Causse A, Ursule E, Theillet C. (2000). At least five regions of imbalance on 6q in breast tumors, combining losses and gains. *Genes Chromosomes Cancer* **27**: 76–84.

Rossmanith W, Chabicovsky M, Grasl-Kraupp B, Peter B, Schausberger E, Schulte-Hermann R. (2002). Follistatin overexpression in rodent liver tumors: a possible mechanism to overcome activin growth control. *Mol Carcinog* **35**: 1–5.

Saito S, Sirahama S, Matsushima M, Suzuki M, Sagae S, Kudo R *et al.* (1996). Definition of a commonly deleted region in ovarian cancers to a 300-kb segment of chromosome 6q27. *Cancer Res* **56**: 5586–5589.

Schwall RH, Robbins K, Jardieu P, Chang L, Lai C, Terrell TG. (1993). Activin induces cell death in hepatocytes *in vivo* and *in vitro*. *Hepatology* **18**: 347–356.

Seglen PO. (1976). Preparation of isolated rat liver cells. *Methods Cell Biol* **13**: 29–83.

Shimura H, Hattori N, Kubo S, Mizuno Y, Asakawa S, Minoshima S *et al.* (2000). Familial Parkinson disease gene product, parkin, is a ubiquitin-protein ligase. *Nat Genet* **25**: 302–305.

Takabe K, Wang L, Leal AM, Macconell LA, Wiater E, Tomiya T *et al.* (2003). Adenovirus-mediated overexpression of follistatin enlarges intact liver of adult rats. *Hepatology* **38**: 1107–1115.

Takahashi R, Imai Y, Hattori N, Mizuno Y. (2003). Parkin and endoplasmic reticulum stress. *Ann NY Acad Sci* **991**: 101–106.

Tanaka Y, Marusawa H, Seno H, Matsumoto Y, Ueda Y, Kodama Y *et al.* (2006). Anti-viral protein APOBEC3G is induced by interferon-a stimulation in human hepatocytes. *Biochem Biophys Res Commun* **341**: 314–319.

Tibiletti MG, Bernasconi B, Furlan D, Riva C, Trubia M, Buraggi G *et al.* (1996). Early involvement of 6q in surface epithelial ovarian tumors. *Cancer Res* **56**: 4493–4498.

Toda Y, Kono K, Abiru H, Kokuryo K, Endo M, Yaegashi H *et al.* (1999). Application of tyramide signal amplification system to immunohistochemistry: a potent method to localize antigens that are not detectable by ordinary method. *Pathol Int* **49**: 479–483.

Trent JM, Stanbridge EJ, McBride HL, Meese EU, Casey G, Araujo DE *et al.* (1990). Tumorigenicity in human melanoma cell lines controlled by introduction of human chromosome 6. *Science* **247**: 568–571.

Von Coelln R, Thomas B, Savitt JM, Lim KL, Sasaki M, Hess EJ *et al.* (2004). Loss of locus coeruleus neurons and reduced startle in parkin null mice. *Proc Natl Acad Sci USA* **101**: 10744–10749.

Wang F, Denison S, Lai JP, Philips LA, Montoya D, Kock N *et al.* (2004). Parkin gene alterations in hepatocellular carcinoma. *Genes Chromosomes Cancer* **40**: 85–96.

West AB, Dawson VL, Dawson TM. (2005). To die or grow: Parkinson's disease and cancer. *Trends Neurosci* **28**: 348–352.

Willert J, Epping M, Pollack JR, Brown PO, Nusse R. (2002). A transcriptional response to Wnt protein in human embryonic carcinoma cells. *Bio Med Central Dev Biol* **2**: 8.

Supplementary Information accompanies the paper on the Oncogene website (http://www.nature.com/onc)

J Neuropathol Exp Neurol

Vol. 67, No. 10
October 2008
pp. 984–993

ORIGINAL ARTICLE

Accumulation of HtrA2/Omi in Neuronal and Glial Inclusions in Brains With α-Synucleinopathies

Yasuhiro Kawamoto, MD, PhD, Yoshito Kobayashi, MD, Yasuyuki Suzuki, PhD, Haruhisa Inoue, MD, PhD, Hidekazu Tomimoto, MD, PhD, Ichiro Akiguchi MD, PhD, Herbert Budka, MD, PhD, L. Miguel Martins, PhD, Julian Downward, PhD, and Ryosuke Takahashi, MD, PhD

Abstract

HtrA2/Omi is a mitochondrial serine protease that is released into the cytosol and promotes apoptotic processes by binding to several members of the inhibitors of apoptosis protein family. HtrA2/Omi knockout mice show a parkinsonian phenotype, and mutations in the gene encoding HtrA2/Omi have been identified as susceptibility factors for Parkinson disease (PD). These results suggest that HtrA2/Omi may be involved in the pathogenesis of PD. We performed immunohistochemical studies of HtrA2/Omi on brains from patients with α-synuclein-related disorders, including PD, dementia with Lewy bodies (DLB), and multiple-system atrophy (MSA); patients with other neurodegenerative diseases; and controls. HtrA2/Omi is expressed in normal brain tissue, and there was some anti-HtrA2/Omi immunostaining of neurons in normal brains as well as those with other neurodegenerative diseases. In PD and DLB brains, both classic (i.e. brainstem-type) and cortical Lewy bodies were intensely immunostained; pale bodies were also strongly immunopositive for HtrA2/Omi. In MSA brains, numerous glial cytoplasmic inclusions, neuronal cytoplasmic inclusions, and dystrophic neurites were also intensely immunoreactive for HtrA2/Omi. These results suggest that widespread accumulation of HtrA2/Omi may occur in pathologic α-synuclein-containing inclusions in brains with PD, DLB, or MSA and that HtrA2/Omi may be associated with the pathogenesis of α-synucleinopathies.

From the Department of Neurology (Y. Kawamoto, Y. Kobayashi, HI, HT, RT), Faculty of Medicine, Kyoto University; Department of Neurology (Y. Kawamoto), Seijinnkai Rakusaisimizu Hospital, Kyoto; and Department of Degenerative Neurological Diseases (YS), National Institute of Neuroscience, National Center of Neurology and Psychiatry, Tokyo, Japan; Center of Neurological and Cerebrovascular Diseases (IA), Koseikai Takeda Hospital, Kyoto, Japan; Institute of Neurology (HB), Medical University of Vienna, Vienna, Austria; Cell Death Regulation Laboratory (LMM), MRC Toxicology Unit, Leicester, UK; and Signal Transduction Laboratory (JD), Cancer Research UK London Research Institute, London, UK.

Send correspondence and reprint requests to: Yasuhiro Kawamoto, MD, PhD, Department of Neurology, Faculty of Medicine, Kyoto University, 54 Shogoin-Kawaharacho, Sakyoku, Kyoto 606-8507; E-mail: kawamoto@kuhp.kyoto-u.ac.jp

This work was supported by a grant from the Ministry of Education, Culture, Sports, Science and Technology of Japan, and by a Grant-in-Aid for Scientific Research on Priority Areas from the Ministry of Education, Culture, Sports, Science and Technology of Japan.

Key Words: α-Synucleinopathy, Glial cytoplasmic inclusions, HtrA2/Omi, Immunohistochemistry, Lewy bodies.

INTRODUCTION

Missense mutations of the α-synuclein gene (*PARK1*) (1–3) and multiplications of the α-synuclein gene (*PARK4*) (4–6) have been reported to be implicated in autosomal dominant familial forms of Parkinson disease (PD). Lewy bodies (LBs) are neuronal inclusions characteristic for PD and dementia with LBs (DLB) (7–9), and α-synuclein has been confirmed to be a major constituent of LBs in PD and DLB (10–12). Multiple-system atrophy (MSA) is a single nosologic entity that encompasses olivopontocerebellar atrophy, striatonigral degeneration, and Shy-Drager syndrome (13). Specific oligodendroglial cytoplasmic inclusions, referred to as *glial cytoplasmic inclusions* (GCIs), are the major pathologic features of brains with MSA (14, 15). α-Synuclein is also a major component of GCIs (12, 16, 17). Therefore, PD, DLB, and MSA are now collectively referred to as *α-synucleinopathies* (18).

The inhibitor of apoptosis protein (IAPs) play an important role in regulating apoptosis; some IAP family proteins, such as X chromosome-linked IAP, have the ability to bind to and directly inhibit selected caspases (19–21). HtrA2/Omi was identified as a mitochondrial serine protease that interacts with IAPs and contributes to the progression of apoptosis (22–25). HtrA2/Omi is released from the mitochondrial intermembrane space into the cytosol upon receiving various apoptotic stimuli, and this released HtrA2/Omi induces apoptotic cell death by binding to IAPs, including X chromosome-linked IAP, and blocking their caspase-inhibitory activities (22–27). HtrA2/Omi also enhances caspase activity by inducing permeabilization of the mitochondrial outer membrane, which leads to the release of cytochrome c (28). Furthermore, HtrA2/Omi knockout mice were reported to show a parkinsonian phenotype, with selective neuronal loss in the striatum (29). Together, these data suggest that, like cytochrome c, HtrA2/Omi is important for cell survival within the mitochondria and that, when it is released from the mitochondria, HtrA2/Omi promotes apoptotic cell death.

Recently, a G399S mutation of the *HtrA2/Omi* gene was identified in some patients with PD, and an A141S

polymorphism of the *HtrA2/Omi* gene was also shown to be associated with PD. These data suggest that HtrA2/Omi is a susceptible factor for PD (PARK13 locus) (30). The results from the targeted disruption of HtrA2/Omi in mice and a mutation screening for HtrA2/Omi in humans suggest that a loss of the function of HtrA2/Omi may be involved in the pathogenesis of PD, but the relationship between HtrA2/Omi and PD remains unclear. In the present study, we performed immunohistochemical studies on HtrA2/Omi using autopsied brains from patients with α-synucleinopathies, including PD. We investigated the detailed neuroanatomic localization of HtrA2/Omi in these diseased brains and found strong HtrA2/Omi immunoreactivity in the α-synuclein-containing inclusions in PD, DLB, and MSA.

MATERIALS AND METHODS

Tissue Preparation

Brains from autopsies of 8 control subjects without any neurologic abnormalities (age range, 54–78 years; mean, 68.4 years; 6 men and 2 women), 10 patients with PD (age range, 66–90 years; mean, 77.5 years; 6 men and 4 women), 5 patients with DLB (age range, 69–86 years; mean, 74.8 years; 4 men and 1 woman), 10 patients with MSA (age range, 52–78 years; mean, 69.1 years; 4 men and 6 women), 5 patients with Alzheimer disease (AD) (age range, 67–85 years; mean, 75.2 years; 1 man and 4 women), a patient with frontotemporal dementia with parkinsonism linked to chromosome 17 (54-year-old man), and a patient with frontotemporal lobar degeneration with ubiquitin-positive inclusions (66-year-old woman). These materials were selected from the brain banks at the Neuropathology Laboratories of Kyoto University and Medical University of Vienna. In 5 of 10 patients with MSA, the MSA was classified as cerebellar variant, and in the other 5 patients, MSA of the parkinsonian variant. The clinical profiles from all cases are summarized in Table 1. All brains were fixed in 10% neutral formalin for about 2 weeks at room temperature. Several paraffin-embedded tissue blocks, including the frontal and temporal cortices, basal ganglia, brainstem, and cerebellum, were prepared and cut into 6-μm-thick sections on a microtome. Sections were deparaffinized in xylene, followed by rehydration in a decreasing concentration of ethanol solutions. For routine pathologic evaluation, the sections from all cases were stained with hematoxylin and eosin (H&E), Klüver-Barrera, and modified Bielschowsky methods. No histologic abnormalities were detected in the sections from any of the control cases. A loss of dopaminergic neurons associated with the presence of classic (brainstem-type) LBs was observed in the substantia nigra from both PD and DLB cases. In addition, many cortical LBs were found in the cerebral cortical regions of the DLB cases, and diagnoses of DLB cases were made according to revised criteria (31). Numerous GCIs were detected in the sections from all of the MSA cases.

Immunohistochemistry

To examine the immunohistochemical localization of HtrA2/Omi, we used an anti-HtrA2/Omi anti-serum raised by immunizing rabbits with *Escherichia coli* expressing the C-terminal His_6-tagged mature form of human HtrA2/Omi protein (22). The deparaffinized sections were pretreated with 0.3% hydrogen peroxide (Santoku, Tokyo, Japan) in

TABLE 1. Case Materials

Case	Age, year/ Sex	Major Diagnosis	Duration of Neurologic Illness, year/Postmortem Delay, hour
Control 1	62/M	Pancreatic carcinoma	NA/3.0
Control 2	68/M	Rheumatoid arthritis	NA/2.0
Control 3	73/M	Hepatocellular carcinoma	NA/4.5
Control 4	68/F	Breast cancer	NA/2.5
Control 5	75/M	Pulmonary emphysema	NA/2.0
Control 6	69/M	Lung cancer	NA/UD
Control 7	54/M	Pneumonia	NA/2.0
Control 8	78/F	Chronic renal failure	NA/9.8
PD 1	90/F	PD	9/2.0
PD 2	76/M	PD	14/2.5
PD 3	79/F	PD	13/1.5
PD 4	81/F	PD	8/2.5
PD 5	74/M	PD	20/UD
PD 6	66/M	PD	10/2.3
PD 7	76/M	PD	8/1.3
PD 8	88/M	PD	10/2.1
PD 9	67/M	PD	17/UD
PD 10	78/F	PD	11/12.0
DLB 1	81/M	DLB	UD/9.0
DLB 2	69/M	DLB	9/11.5
DLB 3	69/F	DLB	27/1.0
DLB 4	69/M	DLB	2/7.5
DLB 5	86/M	DLB	3/5.3
MSA 1	78/M	MSA-C	7/4.8
MSA 2	66/M	MSA-C	4/3.5
MSA 3	72/F	MSA-C	5/2.0
MSA 4	78/M	MSA-C	3/1.8
MSA 5	67/F	MSA-C	2/UD
MSA 6	52/F	MSA-P	3/2.5
MSA 7	77/F	MSA-P	5/1.4
MSA 8	69/F	MSA-P	8/6.1
MSA 9	72/F	MSA-P	12/1.2
MSA 10	60/M	MSA-P	6/3.5
OD 1	80/F	AD	UD/UD
OD 2	85/M	AD	10/UD
OD 3	67F	AD	5/4.2
OD 4	77/F	AD	9/1.4
OD 5	67/F	AD	8/5.9
OD 6	54/M	FTDP-17	8/6.0
OD 7	66/F	FTLD-U	UD/2.9

PD, Parkinson disease; DLB, dementia with Lewy bodies; MSA, multiple-system atrophy; OD, other disease; M, male; F, female; MSA-C, MSA of the cerebellar variant; MSA-P, MSA of the parkinsonian variant; AD, Alzheimer disease; FTDP-17, frontotemporal dementia with parkinsonism linked to chromosome 17; FTLD-U, frontotemporal lobar degeneration with ubiquitin-positive inclusions; NA, not applicable; UD, undetermined.

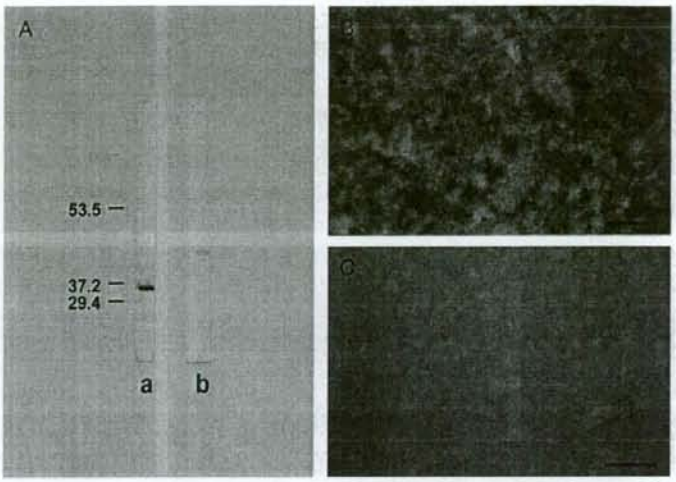

FIGURE 1. Characterization of anti-HTrA2/Omi anti-serum. **(A)** Western blot analysis of normal human brain homogenate. Membranes were incubated with the anti-HtrA2/Omi anti-serum (a) or preimmune serum (b) (see Materials and Methods). The molecular weights (in kilodaltons) are shown to the left. **(B, C)** Immunoreactivities in 20-μm cryosections of frontal cortices of wild-type control **(B)** and knockout **(C)** mice. Scale bars = 50 μm.

0.1 M phosphate-buffered saline (PBS) for 30 minutes at room temperature to inhibit endogenous peroxidase activity. After washing with 0.1 M PBS, the sections were blocked with 0.1 M PBS with 3% skim milk for 2 hours at room temperature. After rinsing with 0.1 M PBS, the anti-HtrA2/Omi anti-serum diluted in 0.1 M PBS (1:200) was applied onto the sections, and they were incubated at room temperature overnight in a humidified chamber. After washing with 0.1 M PBS, the sections were reacted with a biotinylated anti-rabbit immunoglobulin G (IgG; Vector Laboratories, Burlingame, CA) diluted in 0.1 M PBS (1:200) for 1 hour at room temperature, followed by incubation with an avidin-biotin-peroxidase complex (ABC) kit (Vector Laboratories) diluted in 0.1 M PBS (1:400) for 1 hour at room temperature. After rinsing with 0.1 M PBS and then 0.05 M Tris-HCl (pH 7.6), the sections were developed in a colorizing solution containing 0.02% diaminobenzidine tetrahydrochloride (Dojin, Kumamoto, Japan), 0.6% ammonium nickel (II) sulfate (Wako, Osaka, Japan), and 0.005% hydrogen peroxide in 0.05 M Tris-HCl (pH 7.6) for 10 minutes at room temperature. Some H&E-stained sections with classic or cortical LBs were photographed, decolorized with 70% ethanol and were then immunostained with the anti-HtrA2/Omi anti-serum using the ABC method described above. As a negative immunohistochemical control, some sections were incubated with a preimmune rabbit serum; no specific staining was detected in these control sections (data not shown).

Double Immunofluorescence Staining

To compare the anatomic distribution of α-synuclein-immunopositive inclusions to that of HtrA2/Omi-immunopositive inclusions in brains with α-synucleinopathies, we performed double-labeling immunohistochemistry using a goat polyclonal anti-α-synuclein antibody (sc-7011; Santa Cruz Biotechnology, Santa Cruz, CA) and the rabbit anti-HtrA2/Omi anti-serum. Some sections from the PD, DLB, and MSA cases were incubated with the combination of the anti-α-synuclein antibody (1:1000) plus the anti-HtrA2/Omi anti-serum (1:200) in 0.1 M PBS at room temperature overnight. After washing with 0.01 M PBS, the sections were reacted with

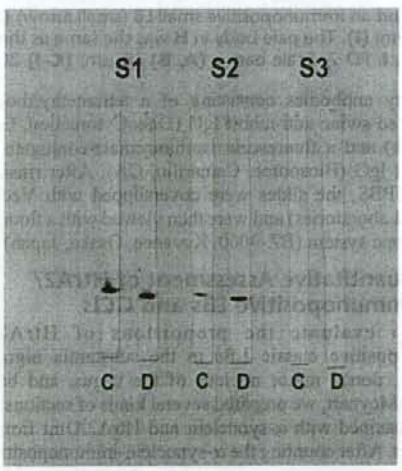

FIGURE 2. Western blot analysis of human brain fractions from control (C) and dementia with Lewy bodies (D) cases. All lanes were incubated with the anti-HtrA2/Omi anti-serum. S1, S2, and S3 indicate phosphate-buffered saline-soluble, sodium dodecyl sulfate-soluble, and formic acid-soluble fractions, respectively.

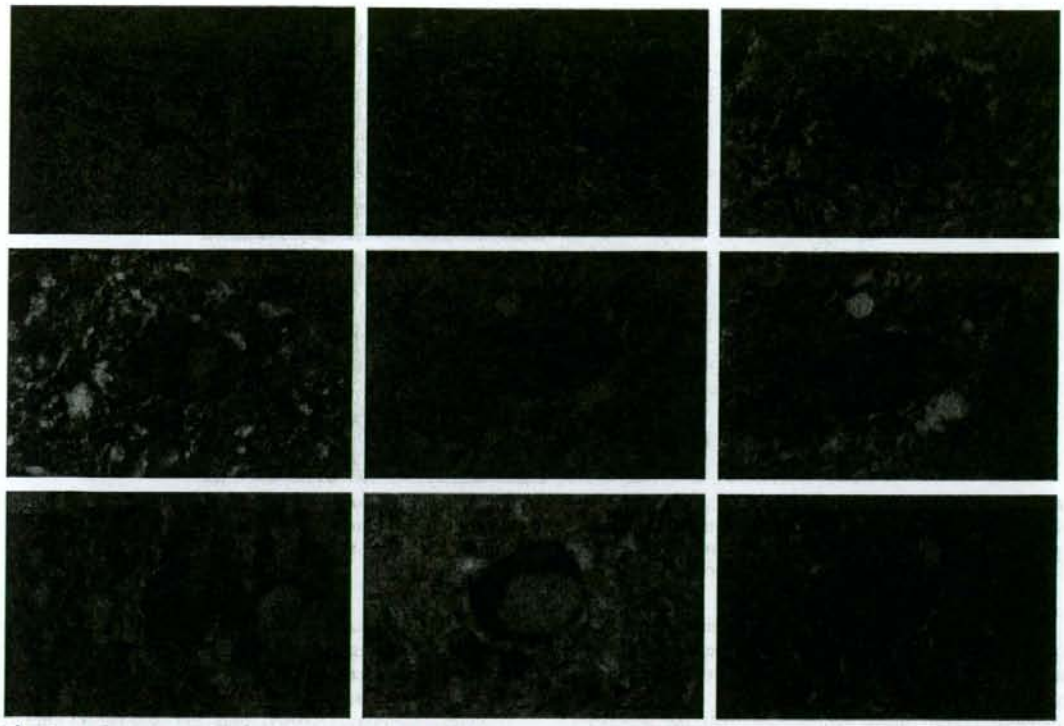

FIGURE 3. Substantia nigra sections stained with H&E and immunostained with the anti-HtrA2/Omi anti-serum. There is a similar immunolabeling pattern in the melanin-containing neurons in the control case **(A)** and in the Parkinson disease (PD) case **(B)**. Classic Lewy bodies (LBs) **(C, E)** show ring-shaped HtrA2/Omi immunolabeling pattern **(D, F)**. The classic LBs in **(C)** and **(E)** are identical to those in **(D)** and **(F)**, respectively. One remaining neuron in a PD case contained an immunopositive large LB (large arrow) and an immunopositive small LB (small arrow) **(G)**. A large, eosinophilic pale body **(H)** is also intensely immunopositive for HtrA2/Omi **(I)**. The pale body in **H** was the same as the one in **I**. Cases illustrated: **A**: Control 3; **B**: PD 3; **C, D**: PD 6; **E, F**: PD 2; **G**: PD 5; **H, I**: PD 7. Scale bars = **(A, B)** 50 μm; **(C–I)** 20 μm.

secondary antibodies consisting of a tetramethylrhodamine-conjugated swine anti-rabbit IgG (DakoCytomation, Glostrup, Denmark) and a fluorescein isothiocyanate-conjugated swine anti-goat IgG (Biosource, Camarillo, CA). After rinsing with 0.01 M PBS, the slides were coverslipped with Vectashield (Vector Laboratories) and were then viewed with a fluorescence microscope system (BZ-9000, Keyence, Osaka, Japan).

Semiquantitative Assessment of HtrA2/Omi-Immunopositive LBs and GCIs

To evaluate the proportions of HtrA2/Omi-immunopositive classic LBs in the substantia nigra, locus ceruleus, dorsal motor nucleus of the vagus, and basal nucleus of Meynert, we prepared several kinds of sections double-immunostained with α-synuclein and HtrA2/Omi from all 10 PD cases. After counting the α-synuclein-immunopositive classic LBs in these areas, we counted the double-immunolabeled classic LBs in the same areas. We then calculated the percentage of HtrA2/Omi-immunopositive classic LBs in each section and the average percentages of HtrA2/Omi-positive classic LBs in the substantia nigra, locus ceruleus, dorsal motor nucleus of the vagus, and basal nucleus of Meynert.

To estimate the proportions of HtrA2/Omi-immunopositive cortical LBs in DLB and GCIs in MSA, we prepared double-immunostained sections with α-synuclein and HtrA2/Omi from all of the DLB and MSA cases. Using the same counting method, we calculated the average percentages of HtrA2/Omi-positive cortical LBs in the superior frontal, cingulate, insular, and parahippocampal cortices and the average percentages of HtrA2/Omi-positive GCIs in the internal capsule, putamen, middle cerebellar peduncle, and cerebellar white matter.

Characterization of the Primary Anti-Serum

The specificity of the anti-HtrA2/Omi anti-serum was confirmed by Western blotting using human brain homogenates. Fresh brain tissues were obtained from the frontal cortex of an autopsied normal subject (68-year-old man). These materials were homogenized in 3 volumes of ice-cold 10 mM PBS containing 1% Nonidet P-40 (Nacalai Tesque, Kyoto, Japan), 0.5% sodium deoxycholate (Difco, Detroit, MI), 0.1% sodium dodecyl sulfate (SDS; Nacalai Tesque), 0.01% phenylmethylsulfonyl fluoride (Nacalai Tesque), 3% aprotinin (Sigma, St Louis, MO), and 1 mM sodium orthovanadate (Sigma). The

homogenates were then centrifuged at 15,000 revolutions per minute (r.p.m.) for 15 minutes at 4°C, and the supernatants were then mixed with an equivalent volume of electrophoresis sample buffer containing 10% glycerol (Nacalai Tesque), 2% SDS, 5% 2-mercaptoethanol (Nacalai Tesque), and 0.00125% bromophenol blue (Nacalai Tesque) in 62.5 mM Tris-HCl (pH 6.8). All samples were then heated for 3 minutes at 100°C and then cooled to room temperature. A 10-μL aliquot of the sample was loaded onto each lane of Mini-Protean II Ready Gels J (Bio-Rad, Hercules, CA), electrophoresed at a constant voltage of 200 V, and then transferred onto polyvinylidene diflouride membranes (Bio-Rad) at a constant voltage of 100 V. After blocking the nonspecific reactions with 3% skim milk plus normal goat serum in 25 mM Tris-buffered saline (TBS), the membranes were incubated with the anti-HtrA2/Omi serum (1:5000) or preimmune serum (1:5000) in 25 mM TBS plus 3% skim milk for 4 hours at room temperature. After washing with 25 mM TBS containing 0.1% Tween 20 (Bio-Rad), the membranes were reacted with an alkaline phosphatase-labeled anti-rabbit IgG (Vector, 1:1000) in 25 mM TBS with 3% skim milk for 1 hour at room temperature. After rinsing with 25 mM TBS containing 0.1% Tween 20, the primary antibodies were visualized using a 5-bromo-4-chloro-3-indolyl-phosphate/nitroblue tetrazolium kit (Nacalai Tesque).

We also performed immunohistochemical studies on HtrA2/Omi using HtrA2/Omi knockout mouse brain sections as a negative control. Brain tissues of knockout and wild-type control mice (both of which have been previously described [29]) were fixed in 10% neutral formalin, stored in 20% sucrose in 0.1 M phosphate buffer, and then cut into 20-μm-thick sections on a freezing microtome. Free-floating sections were immunostained with the anti-HtrA2/Omi serum (1:5000) using the ABC method described above.

Brain Tissue Fractionation

Human brain homogenates were divided into 3 fractions based on their solubility in PBS, SDS, and formic acid. Fresh frontal cortical tissue samples from a control subject (68-year-old man) and a patient with DLB (77-year-old man) were homogenized in 3 volumes of ice-cold 10 mM PBS containing 1% Nonidet P-40, 0.5% sodium deoxycholate, 0.1% SDS, 0.01% phenylmethylsulfonyl fluoride, 3%

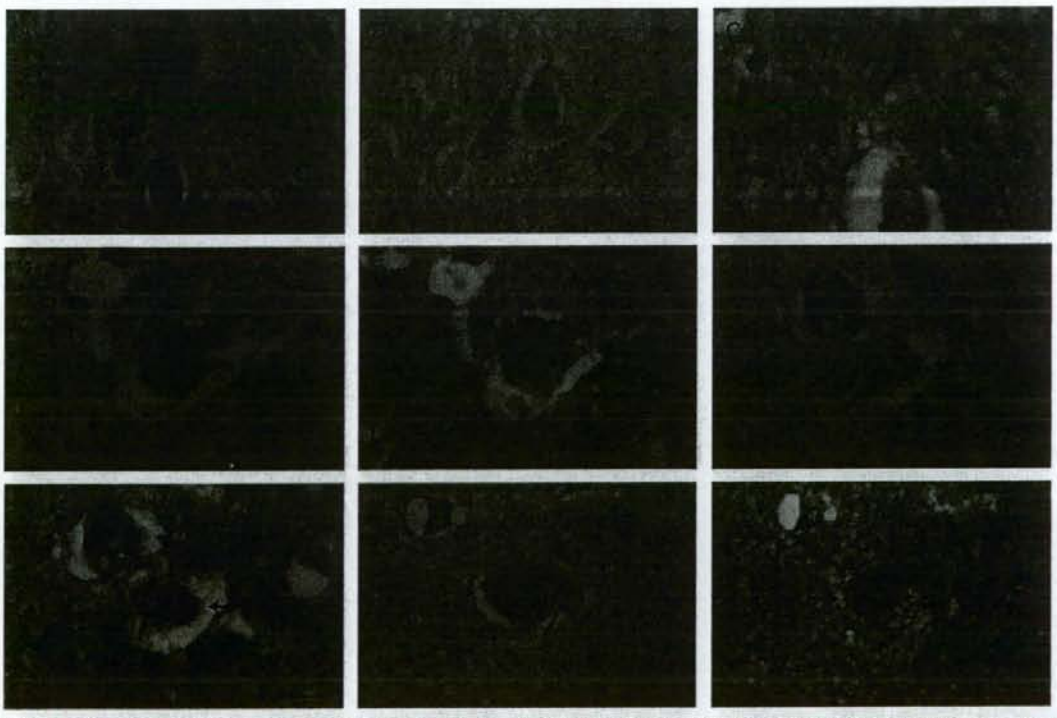

FIGURE 4. Cerebral cortical sections stained with H&E and immunostained with the anti-HtrA2/Omi anti-serum. In the hippocampus from normal controls, there was mild to moderate immunoreactivity in the pyramidal neurons, some of which had densely immunostained perinuclear regions **(A,** arrows**)**. In the hippocampus from patients with dementia with Lewy bodies (DLB), there was strong HtrA2/Omi immunoreactivity in some pyramidal neurons **(B)** and in a few Lewy neurites **(C)**. Cortical Lewy bodies (LBs) consisting of poorly defined, eosinophilic structures with no clear cores and halos **(D, F, H)** showed HtrA2/Omi immunoreactivity **(E, G, I)**. The cortical LBs (arrows) in **(D, F)** and **(H)** are the same as those in **(E, G)** and **(I)**, respectively. Cases illustrated: **A**: Control 4; **B, C, F, G**: DLB 1; **D, E**: DLB 2; **H, I**: DLB 5. Scale bars = 20 μm.

aprotinin, and 1 mM sodium orthovanadate. Each homogenate was centrifuged at 2,500 r.p.m. for 10 minutes at 4°C, and the supernatant was subsequently centrifuged at 55,000 r.p.m. for 1 hour at 4°C, yielding the supernatant (S1, PBS-soluble fraction) and pellet (P1). After washing with 10 mM PBS containing same additives (Buffer A), the P1 pellet was extracted with Buffer A containing 2% SDS and then centrifuged at 55,000 r.p.m. for 1 hour at 4°C, yielding the supernatant (S2, SDS-soluble fraction) and pellet (P2). After rinsing with Buffer A, the P2 pellet was extracted 70% formic acid and then centrifuged at 55,000 r.p.m. for 1 hour at 4°C. The formic acid extract was dried, and the residue was dissolved in Buffer A (S3, formic acid-soluble fraction). All fractions were analyzed using Western blotting with the anti-HtrA2/Omi anti-serum as described above.

RESULTS

Western Blot Analysis

In normal human brain homogenates, the anti-HtrA2/Omi anti-serum immunostained a single band at a molecular weight of approximately 36 kd (Fig. 1A). This corresponds to the molecular weight of the mature form of human HtrA2/Omi and indicates that the anti-serum recognizes HtrA2/Omi in human brain tissues. No specific immunopositive bands were detected in the membrane incubated with the preimmune serum (Fig. 1A). HtrA2/Omi immunoreactivity was detected in the S1 and S2 fractions from control and DLB brains, but the S3 fractions from both showed no HtrA2/Omi immunoreactivity on Western blot (Fig. 2).

HtrA2/Omi Immunoreactivities in Normal and Knockout Mice Brains

HtrA2/Omi immunoreactivity was observed in several types of neurons in the wild-type control mouse brain sections (Fig. 1B), but no specific immunopositive staining was found in the knockout mouse brain sections (Fig. 1C).

HtrA2/Omi Immunoreactivities in Normal and PD Brains

In the substantia nigra of control subjects, melanin-containing neurons generally showed mild to moderate HtrA2/Omi immunoreactivity (Fig. 3A). A similar

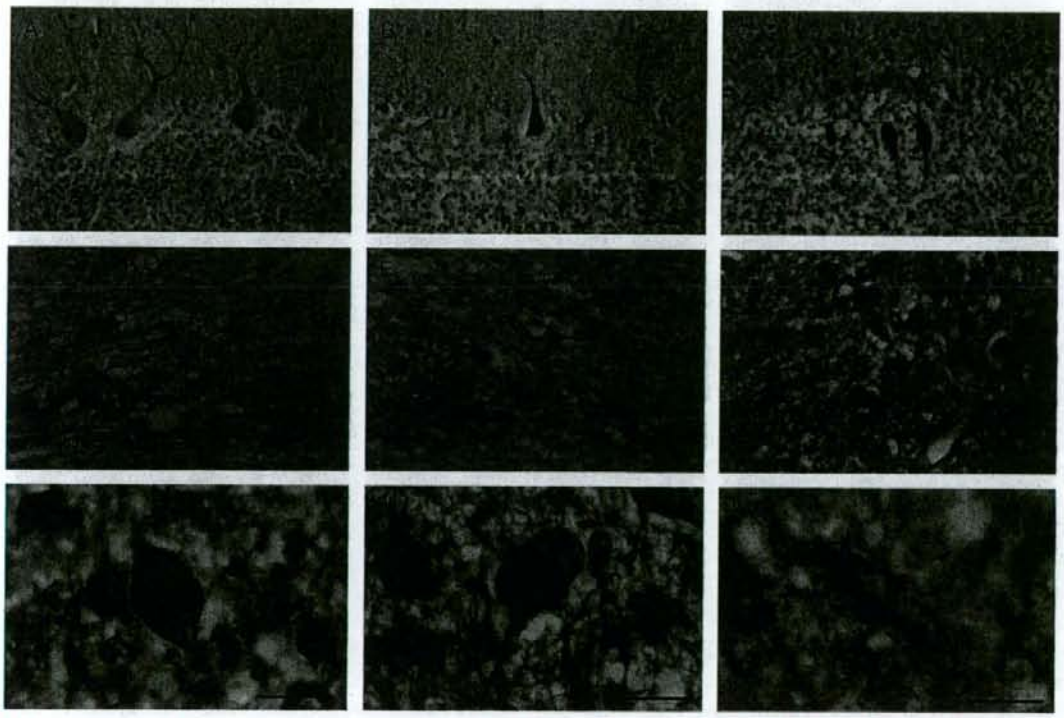

FIGURE 5. HtrA2/Omi immunoreactivity in normal **(A)** and multiple-system atrophy (MSA) **(B–I)** cases. Immunolabeling patterns of the Purkinje cells were similar in the control **(A)** and MSA cases **(B)**. Several torpedoes were also strongly immunopositive for HtrA2/Omi **(C)**. Numerous immunopositive glial cytoplasmic inclusions (GCIs) were found in the pontine nucleus **(D)**, cerebellar white matter **(E)**, and putamen **(F)**. In addition to the GCIs, neuronal cytoplasmic inclusions in the pontine base (**G** arrow, **H** arrow) and swollen neurites in the thalamus **(I)** were also immunoreactive for HtrA2/Omi. Cases illustrated: **A**: Control 1; **B, C, E**: MSA 3; **D, G, I**: MSA 2; **F**: MSA 6; **H**: MSA 7. Scale bars = **(A–C)** 50 μm; **(D–I)** 20 μm.

immunolabeling pattern was observed in the remaining neurons of the substantia nigra from patients with PD (Fig. 3B).

Classic LBs, which generally consist of an eosinophilic core plus a surrounding pale halo (Figs. 3C, E), had a ring-shaped HtrA2/Omi immunostaining pattern; dense accumulations of immunoreactive products were also found in the halos of these LBs (Figs. 3D, F). Some remaining neurons contained 2 or more HtrA2/Omi-immunopositive LBs (Fig. 3G). Pale bodies, which are well-defined, less eosinophilic structures (Fig. 3H), were also heterogeneously immunolabeled (Fig. 3I) and had abundant granular HtrA2/Omi immunoreactivity in their peripheries (Fig. 3I). HtrA2/Omi-immunopositive classic LBs were also found in neurons of the locus ceruleus, dorsal motor nucleus of the vagus, and nucleus basalis of Meynert (not shown).

HtrA2/Omi Immunoreactivities in Normal and DLB Brains

Neurons and glial cells, including oligodendrocytes, of the neocortices and hippocampus in normal controls showed mild to moderate HtrA2/Omi immunoreactivity, and some neurons had strong perinuclear immunoreactivity (Fig. 4A).

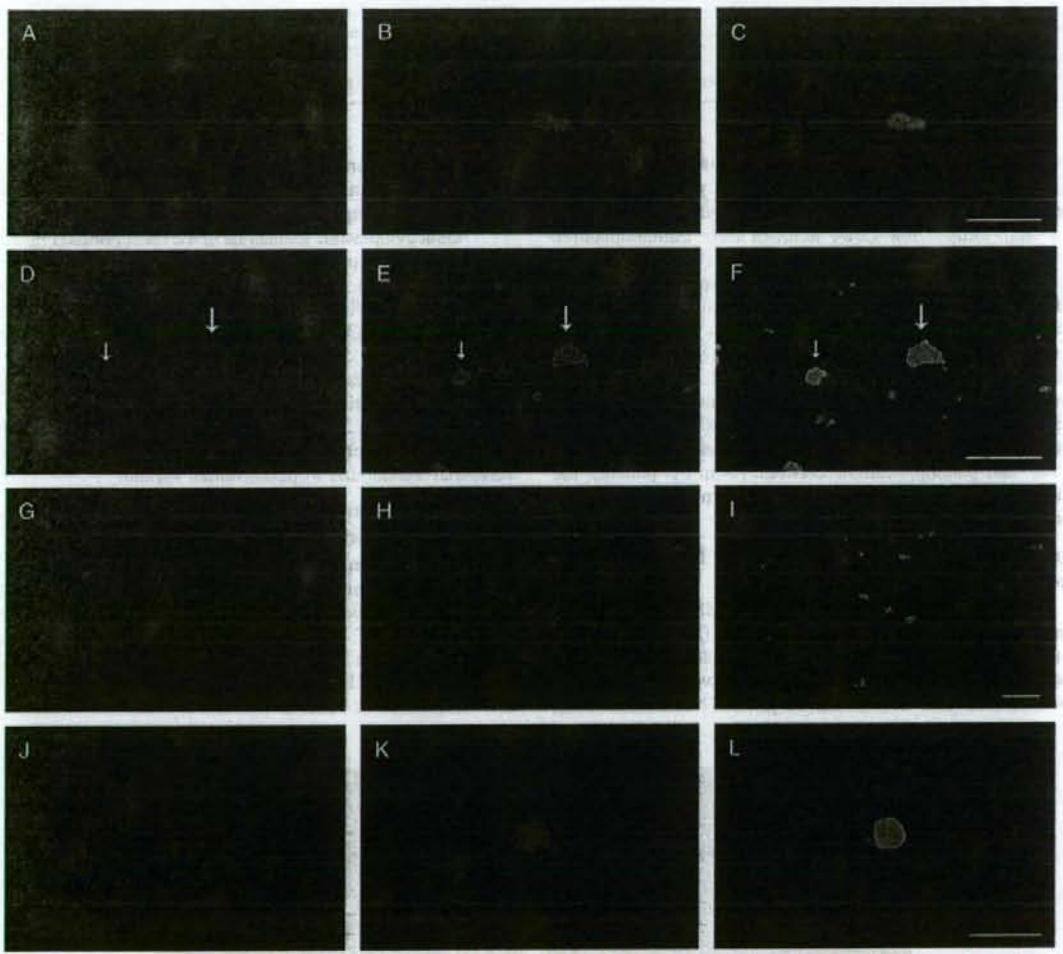

FIGURE 6. Double immunofluorescence staining for HtrA2/Omi **(A, D, G, J)** and α-synuclein **(B, E, H, K)** in the substantia nigra from a patient with Parkinson disease (PD) **(A–C**: PD 2**)**, cingulate gyrus from a patient with dementia with Lewy bodies (DLB) **(D–F**: DLB 4**)** and basis pontis from a patient with multiple system atrophy (MSA) **(G–L**: MSA 2**)**. The merged images showed that HtrA2/Omi and α-synuclein were colocalized in classic Lewy bodies (LBs) **(C)**, cortical LBs **(F)**, glial cytoplasmic inclusions **(I)** and neuronal cytoplasmic inclusions **(L)**. The large and small arrows in **D** to **F** indicate the same cortical LBs, respectively. Scale bars = (**C**, also for **A, B**; **F**, also for **D, E**; **I**, also for **G, H**; **L**, also for **J, K**) 20 μm.

TABLE 2. Summary of HtrA2/Omi-Immunopositive Inclusions

Type of Inclusions	No. Cases Analyzed	Anatomic Localization Evaluated	Average Percentage (%)*
Classic LBs	10 PD	Substantia nigra	68.9
Classic LBs	10 PD	Locus ceruleus	65.5
Classic LBs	10 PD	Dorsal motor nucleus of the vagus	54.9
Classic LBs	10 PD	Basal nucleus of Meynert	62.1
Cortical LBs	5 DLB	Superior frontal cortex	51.1
Cortical LBs	5 DLB	Cingulate cortex	55.8
Cortical LBs	5 DLB	Insular cortex	62.9
Cortical LBS	5 DLB	Parahippocampal cortex	65.7
GCIs	10 MSA	Internal capsule	78.2
GCIs	10 MSA	Putamen	76.9
GCIs	10 MSA	Middle cerebellar peduncle	86.3
GCIs	10 MSA	Cerebellar white matter	79.9

*See Materials and Methods.
LBs, Lewy bodies; GCIs, glial cytoplasmic inclusions; PD, Parkinson disease; DLB, dementia with Lewy bodies; MSA, multiple-system atrophy.

A similar immunolabeling pattern was observed in these regions in DLB patients, immunoreactivity was distributed densely throughout the somata of some remaining neurons (Fig. 4B). Only a few Lewy neurites were immunopositive for HtrA2/Omi (Fig. 4C).

Cortical LBs (i.e. ill-defined, eosinophilic inclusions without a conspicuous core and a clear halo [Figs. 4D, F, H]) were immunopositive for HtrA2/Omi (Figs. 4E, G, I). Some cortical LBs were immunostained diffusely (Fig. 4E), whereas others had partial immunostaining and strongly stained marginal zones (Fig. 4G) or central portions (Fig. 4I). These immunopositive cortical LBs were found throughout the cerebral cortical areas but were more numerous in cingulate, insular, and parahippocampal cortices. As in PD patients, the halos of classic LBs were intensely immunolabeled in DLB patients (not shown).

HtrA2/Omi Immunoreactivities in Normal and MSA Brains

Cerebellar Purkinje cells were mildly to moderately immunostained both in normal subjects (Fig. 5A) and in patients with MSA (Fig. 5B). The torpedoes, which were observed more often in the MSA cases, were also strongly immunopositive for HtrA2/Omi (Fig. 5C). Neuronal labeling patterns in substantia nigra, pontine nuclei, inferior olivary nucleus, and striatum in MSA patients were similar to those in the normal controls.

Glial cytoplasmic inclusions in the basis pontis (Fig. 5D), middle cerebellar peduncle, cerebellar white matter (Fig. 5E), putamen (Fig. 5F), and internal capsule were immunopositive in MSA patients. Strongly immunopositive neuronal cytoplasmic inclusions (NCIs) were found in some remaining neurons of the pons (Figs. 5G, H) and inferior olivary nucleus; a few dystrophic neurites were also densely immunopositive for HtrA2/Omi in various areas, including the basis pontis and thalamus (Fig. 5I). There were no significant differences in the immunolabeling patterns between the cases with MSA of cerebellar variant and of parkinsonian variant.

Double-Labeling Immunohistochemistry for HtrA2/Omi and α-Synuclein

Double-immunostained sections demonstrated HtrA2/Omi and α-synuclein colocalization in many classic LBs (Figs. 6A–C), cortical LBs (Figs. 6D–F), and GCIs (Figs. 6G–I). The colocalization of HtrA2/Omi and α-synuclein was also observed in some NCIs (Figs. 6J–L). Semiquantitative data on percentages of HtrA2/Omi-immunopositive LBs and GCIs are summarized in Table 2.

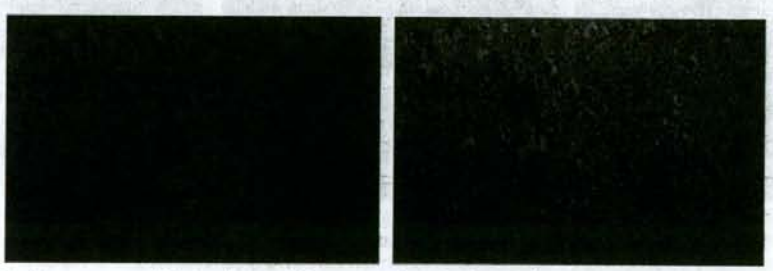

FIGURE 7. HtrA2/Omi immunoreactivity in the parahippocampal cortical areas from patients with Alzheimer disease (**A**: OD 2; **B**: OD 3). Some neurofibrillary tangles **(A)** and dystrophic neurites of senile plaques (**B**, arrows) are immunopositive for HtrA2/Omi. Scale bars = **(A, B)** 20 μm.

HtrA2/Omi Immunoreactivities in Brains With Other Diseases

HtrA2/Omi immunoreactivity was also observed in some neurofibrillary tangles (Fig. 7A) and dystrophic neurites of senile plaques (Fig. 7B) in the brains of patients with AD. By contrast, neuronal and glial inclusions in the case with frontotemporal dementia with parkinsonism linked to chromosome 17 and the case with frontotemporal lobar degeneration with ubiquitin-positive inclusions were immunonegative for HtrA2/Omi.

DISCUSSION

We demonstrate the widespread accumulation of HtrA2/Omi in α-synuclein-containing inclusions in the brains of patients with several types of α-synucleinopathies. To the best of our knowledge, this is the first detailed distribution of HtrA2/Omi immunoreactivity in the brains of these patients. In their study of mutations in the *HtrA2/Omi* gene, Strauss and colleagues (30) referred to the immunohistochemical localization of HtrA2/Omi in classic LBs. We also observed HtrA2/Omi immunoreactivity in the halos of classic LBs and demonstrated HtrA2/Omi immunoreactivity in cortical LBs and pale bodies in patients with PD and DLB, and in GCIs and NCIs in patients with MSA.

Both pale bodies and classic LBs are found in the pigmented neurons of the substantia nigra in patients with PD. Because pale bodies are generally considered to be precursors of classic LBs (9, 32), and both are immunopositive for α-synuclein (9, 12), the presence of HtrA2/Omi as well as of α-synuclein suggests that both may be involved in the formation of classic LBs in the early stages. The immunostaining of pale bodies was heterogeneous, but immunoreaction product was predominantly distributed at their margins. Because the halos of the classic LBs were densely immunopositive, these observations suggest that HtrA2/Omi may accumulate toward the marginal zones of the pale bodies and subsequently form the halos of classic LBs.

Cortical LBs were also immunopositive for HtrA2/Omi, but unlike classic LBs, most cortical LBs did not exhibit a ring-shaped labeling pattern. Some cortical LBs were immunostained diffusely, but HtrA2/Omi immunoreactivity was located mainly at their margins or central portions. Cortical LBs are usually poorly defined eosinophilic structures, and the central cores and peripheral halos usually observed in classic LBs are not evident (8, 9). These differences in structure may contribute to the different HtrA2/Omi-immunostaining patterns.

Since the discovery that 1-methyl-4-phenyl-1,2,3,6-tetrahydropyridine could cause PD-like symptoms in humans (33), several studies have shown that mitochondrial dysfunction plays an important role in the pathogenesis of PD (34). For example, the gene encoding PTEN-induced putative kinase 1 (PINK1) is responsible for PARK6-associated autosomal recessive juvenile parkinsonism (35), and PINK1 has been reported to be localized in the mitochondria (36, 37). Although the immunohistochemical localization of PINK1 in GCIs is controversial (37, 38), PINK1 immunoreactivity has also been found in LBs (37, 38). Recently, HtrA2/Omi was reported to be phosphorylated in a PINK1-dependent manner (39). Because in the present study, we demonstrate the mitochondria-related protein HtrA2/Omi in LBs, interactions between PINK1 and HtrA2/Omi may occur in LBs, and together they may be involved in LB formation.

Mitochondrial dysfunction can lead to apoptotic cell death. There is both neuronal apoptosis in the substantia nigra of patients with PD (40) and oligodendrocyte apoptosis in oligodendrocytes in the brains of patients with MSA (41). Some surviving dopaminergic neurons contain classic LBs in PD (8, 9), and many surviving oligodendrocytes harbor GCIs in MSA (14, 15). Whether these cytoplasmic inclusions induce apoptotic cell death or are protective of these cells from the toxic effects of misfolded proteins remains controversial, but several lines of evidence support the hypothesis that the formation of α-synuclein-containing inclusions may be cytoprotective (42, 43). In the present study, we found that both LBs and GCIs contained dense immunoreactivity for HtrA2/Omi, which in the cytosol might promote apoptosis. Based on these data, we suggest that these inclusions may trap HtrA2/Omi that has been released from the mitochondria and thus protect the dopaminergic neurons in PD and the oligodendrocytes in MSA from HtrA2/Omi-related apoptotic cell death.

A widespread distribution of GCIs in the central nervous system is the main pathologic feature of patients with MSA (14, 15, 44), and α-synuclein is a major component of GCIs (12, 16, 17), but the primary cause of MSA is still undetermined. The intense HtrA2/Omi immunoreactivity observed in GCIs as well as in NCIs and dystrophic neurites in the brains of patients with MSA in the present study suggests that HtrA2/Omi accumulates widely in MSA and that it may be one of the key proteins involved in MSA pathogenesis. Multiple-system atrophy is generally considered to be a sporadic disease, and although familial MSA cases have been identified (45), the genetic factors responsible for MSA remain unclear. Recently, null mutations in the *HtrA2/Omi* gene in mice were shown to lead to parkinsonism accompanied by striatal degeneration (29), a characteristic feature of MSA. Taken together, these results support the possibility that mutations of the gene encoding HtrA2/Omi could be involved in the pathogenesis of MSA. Further genetic analyses on HtrA2/Omi in patients with MSA are necessary.

In conclusion, we found that HtrA2/Omi immunoreactivity accumulated abundantly in brains with α-synucleinopathies, particularly in several types of inclusions containing insoluble α-synuclein, suggesting that HtrA2/Omi may be involved in the aggregation of α-synuclein. Several recent studies have shown that HtrA2/Omi plays an important role in the pathogenesis of AD by regulating β-amyloid precursor protein metabolism (46–48). We also observed the localization of HtrA2/Omi immunoreactivity in some inclusions in brains from patients with AD. These data suggest that HtrA2/Omi may be associated with the pathogenesis of a wide spectrum of neurodegenerative disorders, and further research on the interactions of HtrA2/Omi with α-synuclein will provide new insights into the pathologic mechanisms responsible for α-synucleinopathies.

ACKNOWLEDGMENT

The authors thank Hitomi Nakabayashi for her excellent technical assistance.

REFERENCES

1. Polymeropoulos MH, Lavedan C, Leroy E, et al. Mutation in the α-synuclein gene identified in families with Parkinson's disease. Science 1997;276:2045–47
2. Krüger R, Kuhn W, Müller T, et al. Ala30Pro mutation in the gene encoding α-synuclein in Parkinson's disease. Nat Genet 1998;18: 106–8
3. Zarranz JJ, Alegre J, Gómez-Esteban JC, et al. The new mutation, E46K, of α-synuclein causes Parkinson and Lewy body dementia. Ann Neurol 2004;55:164–73
4. Singleton AB, Farrer M, Johnson J, et al. α-Synuclein locus triplication causes Parkinson's disease. Science 2003;302:841
5. Chartier-Harlin M-C, Kachergus J, Roumier C, et al. α-Synuclein locus duplication as a cause of familial Parkinson's disease. Lancet 2004;364: 1167–69
6. Ibáñez P, Bonnet A-M, Débarges B, et al. Causal relation between α-synuclein gene duplication and familial Parkinson's disease. Lancet 2004;364:1169–71
7. Forno LS, Norville RL. Ultrastructure of Lewy bodies in the stellate ganglion. Acta Neuropathol 1976;34:183–97
8. Pollanen MS, Dickson DW, Bergeron C. Pathology and biology of the Lewy body. J Neuropathol Exp Neurol 1993;52:183–91
9. Takahashi H, Wakabayashi K. The cellular pathology of Parkinson's disease. Neuropathology 2001;21:315–22
10. Spillantini MG, Schmidt ML, Lee VM-Y, et al. α-Synuclein in Lewy bodies. Nature 1997;388:839–40
11. Wakabayashi K, Matsumoto K, Takayama K, et al. NACP, a presynaptic protein, immunoreactivity in Lewy bodies in Parkinson's disease. Neurosci Lett 1997;239:45–48
12. Wakabayashi K, Hayashi S, Kakita A, et al. Accumulation of α-synuclein/NACP is a cytopathological feature common to Lewy body disease and multiple system atrophy. Acta Neuropathol 1998;96: 445–52
13. Graham JG, Oppenheimer DR. Orthostatic hypotension and nicotine sensitivity in a case of multiple system atrophy. J Neurol Neurosurg Psychiatry 1969;32:28–34
14. Papp MI, Kahn JE, Lantos PL. Glial cytoplasmic inclusions in the CNS of patients with multiple system atrophy (striatonigral degeneration, olivopontocerebellar atrophy and Shy-Drager syndrome). J Neurol Sci 1989;94:79–100
15. Nakazato Y, Yamazaki H, Hirato J, et al. Oligodendroglial microtubular tangles in olivopontocerebellar atrophy. J Neuropathol Exp Neurol 1990; 49:521–30
16. Gai WP, Power JHT, Blumbergs PC, et al. Multiple-system atrophy: A new α-synuclein disease? Lancet 1998;352:547–48
17. Wakabayashi K, Yoshimoto M, Tsuji S, et al. α-Synuclein immunoreactivity in glial cytoplasmic inclusions in multiple system atrophy. Neurosci Lett 1998;249:180–82
18. Spillantini MG, Goedert M. The α-synucleinopathies: Parkinson's disease, dementia with Lewy bodies, and multiple system atrophy. Ann N Y Acad Sci 2000;920:16–27
19. Deveraux QL, Takahashi R, Salvesen GS, et al. X-linked IAP is a direct inhibitor of cell-death proteases. Nature 1997;388:300–4
20. Takahashi R, Deveraux Q, Tamm I, et al. A single BIR domain of XIAP sufficient for inhibiting caspases. J Biol Chem 1998;273:7787–90
21. Deveraux QL, Reed JC. IAP family proteins—suppressors of apoptosis. Genes Dev 1999;13:239–52
22. Suzuki Y, Imai Y, Nakayama H, et al. A serine protease, HtrA2, is released from the mitochondria and interacts with XIAP, inducing cell death. Mol Cell 2001;8:613–21
23. Hegde R, Srinivasula SM, Zhang Z, et al. Identification of Omi/HtrA2 as a mitochondrial apoptotic serine protease that disrupts inhibitor of apoptosis protein-caspase interaction. J Biol Chem 2002;277:432–38
24. Martins LM, Iaccarino I, Tenev T, et al. The serine protease Omi/HtrA2 regulates apoptosis by binding XIAP through a Reaper-like motif. J Biol Chem 2002;277:439–44
25. Verhagen AM, Silke J, Ekert PG, et al. HtrA2 promotes cell death through its serine protease activity and its ability to antagonize inhibitor of apoptosis proteins. J Biol Chem 2002;277:445–54
26. Srinivasula SM, Gupta S, Datta P, et al. Inhibitor of apoptosis proteins are substrates for the mitochondrial serine protease Omi/HtrA2. J Biol Chem 2003;278:31469–72
27. Yang Q-H, Church-Hajduk R, Ren J, et al. Omi/HtrA2 catalytic cleavage of inhibitor of apoptosis (IAP) irreversibly inactivates IAPs and facilitates caspase activity in apoptosis. Genes Dev 2003;17:1487–96
28. Suzuki Y, Takahashi-Niki K, Akagi T, et al. Mitochondrial protease Omi/HtrA2 enhances caspase activation through multiple pathways. Cell Death Differ 2004;11:208–16
29. Martins LM, Morrison A, Klupsch K, et al. Neuroprotective role of the Reaper-related serine protease HtrA2/Omi revealed by targeted deletion in mice. Mol Cell Biol 2004;24:9848–62
30. Strauss KM, Martins LM, Plun-Favreau H, et al. Loss of function mutations in the gene encoding Omi/HtrA2 in Parkinson's disease. Hum Mol Genet 2005;14:2099–111
31. Mckeith IG, Dickson DW, Lowe J, et al. Diagnosis and management of dementia with Lewy bodies: Third report of the DLB Consortium. Neurology 2005;65:1863–72
32. Dale GE, Probst A, Luthert P, et al. Relationships between Lewy bodies and pale bodies in Parkinson's disease. Acta Neuropathol 1992;83:525–29
33. Langston JW, Ballard P, Tetrud JW, et al. Chronic Parkinsonism in humans due to a product of meperidine-analog synthesis. Science 1983; 219:979–80
34. Fukae J, Mizuno Y, Hattori N. Mitochondrial dysfunction in Parkinson's disease. Mitochondrion 2007;7:58–62
35. Valente EM, Abou-Sleiman PM, Caputo V, et al. Hereditary early-onset Parkinson's disease caused by mutations in PINK1. Science 2004;304: 1158–60
36. Silvestri L, Caputo V, Bellacchio E, et al. Mitochondrial import and enzymatic activity of PINK1 mutants associated to recessive parkinsonism. Hum Mol Genet 2005;14:3477–92
37. Gandhi S, Muqit MMK, Stanyer L, et al. PINK1 protein in normal human brain and Parkinson's disease. Brain 2006;129:1720–31
38. Murakami T, Moriwaki Y, Kawarabayashi T, et al. PINK1, a gene product of PARK6, accumulates in a-synucleinopathy brains. J Neurol Neurosurg Psychiatry 2007;78:653–55
39. Plun-Favreau H, Klupsch K, Moisoi N, et al. The mitochondrial protease HtrA2 is regulated by Parkinson's disease-associated kinase PINK1. Nat Cell Biol 2007;9:1243–52
40. Mochizuki H, Goto K, Mori H, et al. Histochemical detection of apoptosis in Parkinson's disease. J Neurol Sci 1996;137:120–23
41. Probst-Cousin S, Rickert CH, Schmid KW, et al. Cell death mechanisms in multiple system atrophy. J Neuropathol Exp Neurol 1998;57:814–21
42. Tanaka M, Kim YM, Lee G, et al. Aggresomes formed by α-synuclein and synphilin-1 are cytoprotective. J Biol Chem 2004;279:4625–31
43. Sawada H, Kohno R, Kihara T, et al. Proteasome mediates dopaminergic neuronal degeneration, and its inhibition causes α-synuclein inclusions. J Biol Chem 2004;279:10710–19
44. Papp MI, Lantos PL. The distribution of oligodendroglial inclusions in multiple system atrophy and its relevance to clinical symptomatology. Brain 1994;117:235–43
45. Soma H, Yabe I, Takei A, et al. Heredity in multiple system atrophy. J Neurol Sci 2006;240:107–10
46. Park H-J, Seong Y-M, Choi J-Y, et al. Alzheimer's disease-associated amyloid beta interacts with the human serine protease HtrA2/Omi. Neurosci Lett 2004;357:63–67
47. Park H-J, Kim S-S, Seong Y-M, et al. β-Amyloid precursor protein is a direct cleavage target of HtrA2 serine protease: Implications for the physiological function of HtrA2 in the mitochondria. J Biol Chem 2006; 281:34277–87
48. Huttunen HJ, Guénette SY, Peach C, et al. HtrA2 regulates β-amyloid precursor protein (APP) metabolism through endoplasmic reticulum-associated degradation. J Biol Chem 2007;282:28285–95

パーキンソン病の成因

竹内　啓喜　　高橋　良輔

日本老年医学会雑誌　第44巻　第4号　別刷

老年医学の展望

パーキンソン病の成因

竹内 啓喜　高橋 良輔

要 約 これまでの多くの研究により，パーキンソン病の原因に関して様々な仮説が提唱され，多くのことがわかってきた．その全貌については今なお不明な点も多いが，環境要因と遺伝要因の複合により発症すると考えられている．環境要因については加齢，また農薬や神経伝達物質であるドーパミンが酸化して生じるキノン類等による酸化ストレスの増大，遺伝要因ではミトコンドリア機能に関わるタンパク質や，不要となったり産生の際に異常を来したりしたタンパク質の分解経路，とくにユビキチン—プロテアソーム系の機能不全によるα-シヌクレイン（α-synuclein）の凝集が注目されている．本稿ではこれまでに明らかになったパーキンソン病の発症に関わっていると思われるメカニズムについて，環境要因と遺伝要因それぞれについてまとめた．

Key words：パーキンソン病，農薬，酸化ストレス，α-シヌクレイン，ユビキチン—プロテアソーム系

（日老医誌　2007：44：415–421）

はじめに

パーキンソン病（PD）は，安静時振戦，筋固縮，寡動，姿勢反射障害を4大徴候とする神経変性疾患である．これらの神経学的徴候は中脳黒質のドーパミン作動性神経細胞死によるドーパミン量の低下が直接の原因であり，病理学的にはレビー小体という細胞内封入体を特徴とする．しかし細胞死の原因やレビー小体の成因については，これまでの様々な研究から多くのことが明らかになってきているものの，その全体像については未だ不明である．一般的には，孤発性PDは何らかの遺伝要因と環境要因とが重なってミトコンドリアの機能障害や炎症反応による酸化ストレスの増大，また不要タンパク質の分解処理能が低下して蓄積して生じる細胞毒性でドーパミン作動性神経が細胞死を起こして発症するとされているが，そのメカニズムについては議論が分かれている．そこで孤発性PDと，その研究を大きく前進させることになった家族性PDについてこれまでに示されてきたことを元に，現在考えられているPDの成因についてまとめた．

環境要因

孤発性PDの原因については，これまでの疫学調査で多くのものが候補として挙げられてきた．代表的なものとしては加齢と農薬への曝露で[1]，加齢についてはATP依存性タンパク質分解経路であるユビキチン—プロテアソーム系の機能低下が想定されている[2]．農薬については，農村部での居住，井戸水の利用，農作業への従事がPDのリスクとなっている[3]ことより疑われる一方，PDとよく似た症状をおこす物質が発見されて一部はPDの疾患モデル作製に応用された[4]（表1）．これらは酸化ストレスを増大させることでドーパミン作動性神経に選択的に細胞死を起こし，直接活性酸素種（Reactive oxygen species; ROS）を産生するディルドリン[5]（本邦では製造中止），ミトコンドリア電子伝達系阻害によるものとしてはパラコート，ロテノンなどがある．除草剤として使われるパラコートは可逆的ではあるが，マウス中脳黒質ドーパミン神経内でレビー小体の主要構成成分であるα-synucleinの集簇を促す[6]．ロテノンはマメ科植物の根から得られる天然由来の農薬であるが，慢性投与によりミトコンドリア電子伝達系複合体Iを阻害しラットにPDと似た症状を示すだけでなく黒質から線条体にかけてのドーパミン神経の減少と細胞質内にレビー小体に似た封入体が形成する[7]．これまでの薬物モデルでは封入体形成がみられないことを考えると，ロテノンはPDの病態に近いモデルを作製できる毒物として有用なものと思われる．また農薬とは別にPDモデル作製に使われているものとしてMPTP，6-ヒドロキシドーパミン（6-OHDA）などがある．いずれもドーパミントランスポー

H. Takeuchi, R. Takahashi：京都大学大学院医学研究科臨床神経学（神経内科）

表1　パーキンソン病関連因子とモデル作製に使う毒物

正の相関	モデル作製に使う毒物	負の相関
加齢	6-OHDA	喫煙（ニコチン？）
農村部での居住	MPTP	コーヒー（カフェイン？）
井戸水の使用	ロテノン	
農薬への従事	パラコート	
農薬への曝露	ディルドリン（本邦では使用中止）	

ターによってドーパミン神経に取り込まれることで選択毒性を発揮し，ミトコンドリア電子伝達系複合体Iを阻害し，ROSの産生を上昇させて毒性を発揮する．MPTPは麻薬中毒患者にPD様症状がみられたのをきっかけに合成麻薬の不純物として発見され[8]，PD研究を飛躍させることになった．また，以前より毒物モデル作製に用いられている6-OHDAはドーパミンの水酸化物として得られたものであるが内因性に存在し，ドーパミン神経を傷害する可能性が示唆されている[9]．既に知られている内因性のドーパミン神経毒性を持つ物質としてはドーパミンの自己酸化により生成されるイソキノリン類[10]や，β-カルボリン誘導体[11][12]が知られる．いずれにせよこれらPDとよく似た特徴を示す薬物は，概して酸化ストレス増大を引き起こすものである．なお金属イオン中毒もマンガンを主体に取り上げられているが，既に発症しているPDを悪化させるものの，一次的な原因としての根拠は不十分である[13]．プロテアソーム阻害薬でPDモデル動物を作製したとの報告もあるが[14]，この結果は再現性に問題があることが指摘されている[15][16]．また，逆に保護的であったとの報告もあり[17]，統一した見解は得られていない．

一方，PDと負の相関を持つ因子も調査されており，代表的なものとして喫煙[18]とコーヒー摂取[19]があげられている．いずれもそのメカニズムについてはよくわかっていないが，喫煙については，ニコチンの作用が挙げられており，ニコチン受容体を介して黒質のドーパミン神経からのドーパミン遊離を促す[20]，神経保護効果としてはPI3K-Aktシグナル伝達によりBcl familyを活性化する[21]，あるいはNF-κB抑制によりアポトーシスを抑制する[22]，free radical scavenger作用をもち酸化ストレスを直接減少させる[23]，ミクログリアからの細胞傷害因子放出を抑制する[24]，などが報告されている．またコーヒーは，カフェインがアデノシンA_{2A}受容体を阻害することにより細胞保護効果を示していると考えられている[25]．これらの臨床応用はそのままでは依存性や忍容性，他臓器への影響の面で問題があるため，コリンエステラーゼ阻害薬やニコチン受容体のアゴニスト，他のアデノシンA_{2A}受容体阻害薬の使用が期待される．また，NSAIDsが神経細胞脱落部位での炎症反応を抑制することで神経保護に働くと考えられたが，疫学調査では効果は部分的なようである[26]．

遺伝要因

1．家族性PD

PDは90%が明らかな家族歴のない孤発性で，家族性（即ち遺伝性）のものは5～10%程度と少ない[27]．しかし家族性症例の原因遺伝子を突き止めることが孤発例の原因解明につながるため，PDでも同様に家族例について多くの研究がなされ，その結果PDの発症メカニズムについて多くのことがわかってきた．以下，これまでに原因遺伝子が明らかになった家族性PDとその遺伝子について述べる．主だった特徴については別表にまとめた（表2）．

A．常染色体優性遺伝

PARK1，PARK4はα-synucleinの遺伝子の変異による．表現型は孤発性PDとほぼ同じでL-ドーパも有効だが，発症年齢が40～50代と若年傾向で認知症が目立つ．病理学的所見も孤発性PDと似通っているが，レビー小体が黒質だけでなく皮質でもみられる．これまでに知られている変異は53番目のアラニンがスレオニンに，30番目のアラニンがプロリンに，46番目のグルタミン酸がリジンに（A53T，A30P，E46K）[28]～[30]変異したものであり，これらは正常型より凝集しやすい．α-synucleinの生理機能はシナプス前に存在し，ドーパミン放出や再取り込みにかかわるはたらきを持つことが報告され[31][32]，α-synucleinの機能不全が神経毒性をもつドーパミンの自己酸化生成物を増大させることでドーパミン神経細胞死が生じるのかもしれない[33]．

PARK1の報告例は少ないが，レビー小体の主要成分がユビキチン化やリン酸化を受けたα-synucleinであることが明らかになり，注目を集めるようになった[34]～[36]．α-synucleinが何らかの理由により凝集して細胞毒性を発揮し，ドーパミン神経に選択的に細胞死をおこす，という孤発性PDの発症仮説のもと，様々な遺伝子改変動物がつくられている．ヒト正常型α-synucleinや前述の変異α-synucleinを導入したショウジョウバエではドーパミン作動性神経の減少，レビー小体様の細胞内封入体やα-synucleinのフィブリルが形成され，運動機能障害の表現型がみられるが[37]，マウスでは細胞内封入体やフィブリル形成が見られてもドーパミン作動性神経の脱

表2　家族性パーキンソン病

疾患	遺伝形式	遺伝子座	遺伝子	表現型※	年齢	L-DOPA の効果	レビー小体
PARK1	AD	4q21	α-synuclein	PD + dementia	broad	+	+
PARK2	AR	6q25-27	parkin	PD + dystonia	～40代	+	−
PARK3	AD	2p13	?	PD	60代	+	+
PARK4	AD	4q21	α-synuclein	PD + dementia	30代	+	+
PARK5	AD	4p14	UCH-L1	PD	50代	+	+?
PARK6	AR	1p35	PINK-1	PD + dystonia	30代	+	−?
PARK7	AR	1p36	DJ-1	PD + dystonia	30代	+	?
PARK8	AD	12q12	LRRK2	PD	broad	+	+ or −
PARK9	AR	1p36	ATP13A2	PD +注視制限	10代	+	?
PARK10	AR	1p32	?	PD	60代	+?	?
PARK11	AD	2q36-37	?	PD	60代	?	?
PARK12	X-linked	Xq21-25	?	PD ?	60代	?	?
PARK13	AD	2p12	Omi/HtrA2	PD	50代	+	+?

PD：sporadic PD の表現型　※特徴的所見

落がみられないか，みられてもごく軽度であり，表現型も軽度な異常にとどまっている[38]．これは齧歯類以上のほ乳類ではα-synuclein 凝集以外の要素も重要であることを示唆しているのかもしれない．一方，同じくα-synuclein 遺伝子の変異を原因とするが，正常型遺伝子の三重複が PARK4 である．PARK4 は孤発性 PD 症状に加えて早期から認知症や自律神経障害を伴い，L-ドーパが有効であるが孤発性と比べて若年で発症（30 歳代）し，進行も早い．病理像ではレビー小体が黒質や青斑核のみならず大脳皮質にも広範に見られ，海馬やマイネルト基底核で空胞形成がみられる．しかし，神経原線維変化や老人斑は正常レベルにとどまる[39]．また，α-synuclein 二重複の家系も報告されているが，孤発性 PD と比べて早期に発症するものの臨床症状はあまり変化なく認知症の合併も少ない[40]．これらの所見より，PD 発症にα-synuclein は大変重要な役割を果たしていることが明らかになった．

PARK5 は UCH-L1（Ubiquitin C-terminal hydrolase）遺伝子の変異によるもので，50 歳前後で発症し，臨床症状は孤発性 PD と明らかな違いはなく，L-ドーパが有効である．これまでのところドイツの一家系のみの報告で，93 番目のイソロイシンのメチオニンへの変異（I93M）を認めている[41]．UCH-L1 は脱ユビキチン化酵素の一種で，他の分子と結合したユビキチンの C 末端を切断してユビキチンを活性化し，ユビキチンを供給している[39]ことから I93M の変異でユビキチン供給が低下する結果，異常蛋白が蓄積し，パーキンソン症状をおこすものと考えられている．これまでに剖検例がなくレビー小体の有無は不明であるが，トランスジェニックマウスでは中脳黒質で UCH-L1 の凝集がみられている[42]．

一方 UCH-L1 二量体ではα-synuclein に対するユビキチンリガーゼとして働き，ポリユビキチン化を行う[43]．このときのユビキチン鎖は 26S プロテアソームでの分解のシグナルとなる 48 番目のリジン（K48）ではなく 63 番目のリジン（K63）を介して形成される．その結果α-synuclein が蓄積すると考えられているが，I93M 変異ではユビキチンリガーゼ活性が低下しており，必ずしも発症危険度と相関しない[44]．このプロテアソームでの分解シグナルとならないユビキチン化の意義を明らかにすることが，病因解明の上での大きな鍵であると思われる．

PARK8 は LRRK2（Leucine-Rich Repeat Kinase2）遺伝子の変異による[45]．孤発例と思われていた症例でも変異が見いだされており，浸透率も様々で家族性 PD では最も多いものと思われる[46]．臨床症状はほぼ孤発性 PD と同じであり，発症年齢も多くは 50～60 歳代である．L-ドーパが有効で，臨床経過も他の家族性 PD と比べて比較的良好である．LRRK2 は 2527 アミノ酸からなる分子量 286kDa の巨大分子で，細胞質内やミトコンドリアに存在し，種々のドメインを持ち複数の作用を持つことが予想されている[47]．これまで報告された変異は，MAP キナーゼ—キナーゼ—キナーゼドメイン（MAPKKK）中のものが多く（G2019S，I2020T）[47]，G2019S 変異ではキナーゼ活性の亢進が報告されている[48]．このため何らかのタンパク質の異常なリン酸化が発症につながっていると思われる．本疾患は病理所見が多彩で，MAPKKK ドメインの変異でも G2019S 変異ではレビー小体が見られるが[49]日本の相模原家系の I2020T 変異ではみられないことが多く[50]，病理像を修飾する他因子の関与も疑われる．

B. 常染色体劣性遺伝

PARK2はparkinを原因遺伝子とする若年性パーキンソニズムである．本邦で報告され[51]，かつ原因遺伝子の特定[52]も行われた．変異は種々のエクソンの欠失や[53]点変異が報告されている[54]が，いずれにせよこれらの変異によりユビキチンリガーゼとしての活性が低下するloss-of-function変異である．孤発性PDと比較して，臨床症状においては，1)40歳以下での発症が大半である，2）ジストニアを呈する，3）症状に日内変動を認める，4）睡眠により改善する，5）L-ドーパが有効であるが早期よりジスキネジアを生じる，6）病理所見ではレビー小体を認めない，といった差異がある．また，parkinがS-ニトロシル化を受けて活性が低下することが報告されており，孤発性PDの発症にも関与していると思われる[55][56]．このことからparkinの基質蓄積が発症原因のひとつであるとの仮説の元，さまざまなタンパク質の検索が行われた．中でもPael受容体（Parkin-associated endothelin receptor-like receptor）は[57]，正常な状態でも正しい折りたたみ構造をとることができないものが多く産生されるため（misfoldingしやすい），parkinによるユビキチン化が低下すると蓄積し，小胞体ストレスを増大させる[58]．またPael受容体はレビー小体にも存在し，PD発症に大きな役割を果たしていると思われる[59]．

PARK6はPINK1（PTEN-Induced Kinase1）遺伝子の変異による[60]．30～40代で発症し，臨床症状は孤発性PDと明らかな違いはなくL-ドーパが有効な症例が多いが，より若年での発症においてジスキネジアが多い[61]．PINK1はミトコンドリアに局在しミトコンドリアターゲットモチーフとセリン/スレオニンキナーゼドメインをもち，前者によりミトコンドリア内に移動し，後者よりミトコンドリアにおいて細胞保護的な役割を果たしていると考えられている[60]．これまでに報告されている変異はセリン/スレオニンキナーゼドメインに集中しており[60][62]～[64]，キナーゼ活性が低下する．このためPINK1のキナーゼ活性が発症に重要な役割を果たしていると思われるが，ミトコンドリア電子伝達系複合体Iのサブユニットのいくつかがリン酸化をされていることが報告されており[65]～[68]，両者の関連がうかがわれる[66]．PINK1はレビー小体の構成成分であるが，本例でその存在が報告されているのは現在のところヘテロ変異のみである[69][70]．

PARK7はDJ-1の変異により発症する[71]．20～40代で発症し，孤発性PD症状に加え下肢のジストニアや眼瞼攣縮，精神症状（認知症症状，不安症，妄想など）を呈し[72]，L-ドーパが有効である．一部の症例でジスキネジアもみられる[71]．DJ-1は抗酸化作用[73]，プロテアーゼ活性，転写調節因子と種々の働きをもち[74]，種々の変異が報告されているが，変異により抗酸化作用または酸化ストレスのセンサーとしての働きが失われ[75]，酸化ストレスが増大してドーパミン神経細胞死がおこると考えられている．またL166P変異でDJ-1蛋白の折りたたみ不全が生じ，すみやかにユビキチン―プロテアソーム系で分解されること[76]，parkin基質であるPael受容体による小胞体ストレスが野生型DJ-1にて軽減される[77]ことも合わせると，酸化ストレス以外に想定されるPDの原因への関与も考えられる．DJ-1はレビー小体の構成成分であるが，本例においてレビー小体が存在するかどうかはわかっていない．

PARK9[78][79]はATP13A2遺伝子の変異を原因とする，Kufor-Rakeb病として知られる．10代で発症し孤発性PDの症状に加え，錐体路障害，上方注視制限，認知症症状を合併する．L-ドーパは有効であるが，進行は早い．ATP13A2はP型ATPase（plasma membraneに存在するATPase）の一種で，正常型はリソソームの膜に発現するが，この疾患で見られる変異型は機能低下を来たし，小胞体に集まり，プロテアソームによる分解を受ける．小胞体ストレス増大でのプロテアソーム機能不全，あるいはリソソームでのタンパク分解（オートファジー）低下が神経細胞死の原因となるかどうかは不明であるが，オートファジー不全がPDの発症に関与することを示唆するもので，興味深い知見である．

C. 遺伝子多型

これまでに種々の遺伝子多型とPDの関連が報告されている．代表的なものとしては遺伝子多型にOmi/HtrA2遺伝子[80]がある．これはミトコンドリアのプロテアーゼであり，後に変異が発見された（PARK13）[80]．変異Omi/HtrA2（399番目のグリシンがセリン：G399S）ではプロテアーゼ活性が低下しており，ミトコンドリア機能不全がうかがわれる[80]．また，α-synucleinでもイントロンの遺伝子多型と孤発性PDとの関連が報告されており[81]，splicingの段階での変化も関連しているのかも知れない．

まとめ

これまでに述べたPDの原因と考えられている環境因子，遺伝的要因についてまとめた（図1）．即ちミトコンドリアにおける電子伝達系や各種酵素やタンパク質の機能不全で酸化的ストレスが増大し，ドーパミン神経細胞のアポトーシスを亢進する（ミトコンドリア仮説）．また異常タンパク質が，ユビキチン―プロテアソーム系が何らかの理由（異常蛋白が構造上分解困難，正常な分

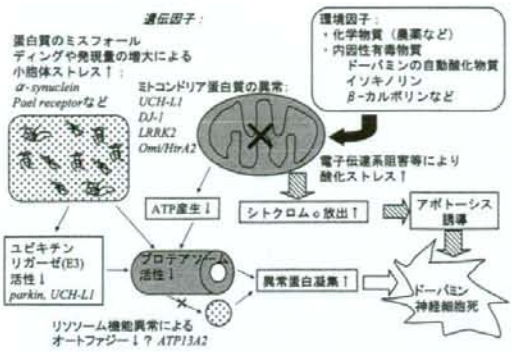

図1　パーキンソン病におけるドーパミン神経細胞死の仮説

解能力を超えて産生される，ミトコンドリア機能低下でATP供給が低下する）で傷害されることで蓄積し細胞毒性を持つ（ユビキチン—プロテアソーム仮説）ことが主な原因と考えられている．また一部，代償的にリソソームで行われるオートファジーの機能不全も関係しているかもしれない．今後，これらの知見をさらに発展させ，根本原因に迫る疾患の予防法や治療法の開発をすすめていくことが期待される．

文　献

1) Di Monte DA, Lavasani M, Manning-Bog AB: Environmental factors in Parkinson's disease. Neurotoxicology 2002; 4-5: 487–502.
2) Martinez-Vicente M, Sovak G, Cuervo AM: Protein degradation and aging. Exp Gerontol 2005; 40 (8-9): 622–633.
3) Priyadarshi A, Khuder SA, Schaub EA, Priyadarshi SS: Environmental risk factors and Parkinson's disease: a metaanalysis. Environ Res 2001; 86 (2): 122–127.
4) Uversky VN: Neurotoxicant-induced animal models of Parkinson's disease: understanding the role of rotenone, maneb and paraquat in neurodegeneration. Cell Tissue Res 2004; 318 (1): 225–241.
5) Kitazawa M, Anantharam V, Kanthasamy AG: Dieldrin-induced oxidative stress and neurochemical changes contribute to apoptotic cell death in dopaminergic cells. Free Radic Biol Med 2001; 31 (11): 1473–1485.
6) Manning-Bog AB, McCormack AL, Li J, Uversky VN, Fink AL, Di Monte DA: The herbicide paraquat causes up-regulation and aggregation of alpha-synuclein in mice: paraquat and alpha-synuclein. J Biol Chem 2002; 277 (3): 1641–1644.
7) Betarbet R, Sherer TB, MacKenzie G, Garcia-Osuna M, Panov AV, Greenamyre JT: Chronic systemic pesticide exposure reproduces features of Parkinson's disease. Nat Neurosci 2000; 12: 1301–1306.
8) Watanabe Y, Himeda T, Araki T: Mechanisms of MPTP toxicity and their implications for therapy of Parkinson's disease. Med Sci Monit 2005; 11 (1): RA17–23.
9) Blum D, Torch S, Lambeng N, Nissou M, Benabid AL, Sadoul R, et al.: Molecular pathways involved in the neurotoxicity of 6-OHDA, dopamine and MPTP: contribution to the apoptotic theory in Parkinson's disease. Prog Neurobiol 2001; 65 (2): 135–172.
10) Naoi M, Maruyama W, Dostert P, Ota M, et al.: Dopamine-derived endogenous 1 (R), 2 (N)-dimethyl-6, 7-dihydroxy-1, 2, 3, 4-tetrahydroisoquinoline, N-methyl-(R)-salsolinol, induced parkinsonism in rat: biochemical, pathological and behavioral studies. Brain Res 1996; 709 (2): 285–295.
11) Matsubara K, Kobayashi S, Kobayashi Y, Yamashita K, Koide H, Kimura K, et al.: beta-Carbolinium cations, endogenous MPP+ analogs, in the lumbar cerebrospinal fluid of patients with Parkinson's disease. Neurology 1995; 45 (12): 2240–2245.
12) Matsubara K, Gonda T, Sawada H, Uezono T, Kobayashi Y, Akaike A: Endogenously occurring beta-carboline induces parkinsonism in nonprimate animals: a possible causative protoxin in idiopathic Parkinson's disease. J Neurochem 1998; 70 (2): 727–735.
13) McMillan G: Is electric arc welding linked to manganism or Parkinson's disease? Toxicol Rev 2005; 24 (4): 237–257.
14) McNaught KS, Olanow CW: Proteasome inhibitor-induced model of Parkinson's disease. Ann Neurol 2006; 60 (2): 243–247.
15) Beal F, Lang A: The proteasomal inhibition model of Parkinson's disease: "Boon or bust"? Ann Neurol 2006; 60 (2): 158–161.
16) Stephen L Hauser: Proteosome inhibitors revisited. Ann Neurol 2006; 60 (2): A10.
17) Inden M, Kondo J, Kitamura Y, Takata K, Nishimura K, Taniguchi T, et al.: Proteasome inhibitors protect against degeneration of nigral dopaminergic neurons in hemiparkinsonian rats. J Pharmacol Sci 2005; 97 (2): 203–211.
18) Wirdefeldt K, Gatz M, Pawitan Y, Pedersen NL: Risk and protective factors for Parkinson's disease: a study in Swedish twins. Ann Neurol 2005; 57 (1): 27–33.
19) Ascherio A, Zhang SM, Hernan MA, Kawachi I, Colditz GA, Willett Wc, et al.: Prospective study of caffeine consumption and risk of Parkinson's disease in men and women. Ann Neurol 2001; 50 (1): 56–63.
20) Morens DM, Grandinetti A, Reed D, White LR, Ross GW: Cigarette smoking and protection from Parkinson's disease: false association or etiologic clue? Neurology 1995; 45: 1041–1051.
21) Kihara T, Shimohama S, Sawada H, Honda K, Nakamizo T, Akaike A: alpha 7 nicotinic receptor transduces signals to phosphatidylinositol 3-kinase to block Aβ-amyloid-induced neurotoxicity. J Biol Chem 2001; 276 (17): 13541–13546.
22) Liu Q, Zhang J, Zhu H, Qin C, Chen Q, Zhao B: Dissecting the signaling pathway of nicotine-mediated neuroprotection in a mouse Alzheimer disease model. FASEB J 2007; 21 (1): 61–73.
23) Xie YX, Bezard E, Zhao BL: Investigating the receptor-independent neuroprotective mechanisms of nicotine in mitochondria. J Biol Chem 2005; 280 (37): 32405–32412.
24) Suzuki T, Hide I, Matsubara A, Hama C, Harada K, Nakata Y, et al.: Microglial alpha7 nicotinic acetylcholine receptors drive a phospholipase C/IP3 pathway and modulate the cell activation toward a neuroprotective role. J Neurosci Res 2006; 83 (8): 1461–1470.
25) Kalda A, Yu L, Oztas E, Chen JF: Novel neuroprotection by caffeine and adenosine A_{2A} receptor antagonists in animal models of Parkinson's disease.
26) Ton TG, Heckbert SR, Longstreth WT Jr, Rossing MA, Kukull WA, Checkoway H: Nonsteroidal anti-inflammatory drugs and risk of Parkinson's disease. Mov Disord 2006; 21 (7): 964–969.